SEPTEMBER 1989

PLASMA DIAGNOSTICS FOR THE RIJNHUIZEN TOKAMAK PROJECT

A.J.H. DONNÉ, S.K. KIM, C.J. BARTH, D.F. DA CRUZ JR., B.J.J. GROBBEN,
B. DE GROOT,   P.C. VAN HAREN,   C.A.J. HUGENHOLTZ,   J.J. KONING,
H.A. VAN DER LAAN, A.C.A.P. VAN LAMMEREN, A.F.G. VAN DER MEER,
G.J.J. REMKES, W. VAN TOLEDO, P.H.M. VAESSEN, G.C.H.M. VERHAAG,
M. VERRECK AND J.M.M. DE WIT

RIJNHUIZEN REPORT 89-187

Contents

1

Abstract

The primary aim of the Rijnhuizen Tokamak Project (RTP) is the study of transport and fluctuations in tokamak plasmas. Therefore, much attention is devoted to attain an as good as possible spatial and temporal resolution as well as a high accuracy for the various diagnostical systems. For the measurement of (fluctuations in) some plasma parameters new techniques have to be developed. A review of the design issues and other aspects impacting the selection of diagnostic techniques for RTP will be presented.

Introduction

To achieve thermonuclear conditions in a tokamak it is necessary to confine the plasma and its energy for a sufficiently long time.[1] The confinement is limited by thermal conduction, particle diffusion and convection processes, and by radiation.[2] For a tokamak plasma having a set of nested toroidal magnetic flux surfaces on which the plasma pressure is close to constant, there is an irreducible loss rate resulting from Coulomb collisions. In a cylindrically symmetric configuration this diffusion process is known as classical transport. The reduced symmetry of a toroidal configuration leads to an enhanced level of transport known as neoclassical transport. For example, it is characteristic of this collisional transport that the ion thermal diffusivity χ_i exceeds the electron thermal diffusivity χ_e by a factor $(m_i/m_e)^{1/2}$. Consequently, collisional transport theory predicts that the energy loss is determined primarily by the ion confinement time $\tau_{Ei} \approx a^2/\chi_i$, with a the minor radius of the plasma. However, detailed analysis of experiments indicates that thermal losses through electrons exceed the neoclassical prediction by up to two orders of magnitude, whereas ion thermal losses are much closer to neoclassical theory.[2] Therefore, in reality ion- and electron heat losses are about equal. These enhanced losses are called anomalous transport.

In order to assess the viability of a tokamak reactor it would clearly be useful to understand the cause of anomalous transport. There are several potential explanations, generally associated with the presence of micro-instabilities.[2] Even if the instabilities preserve the topology of the magnetic surfaces, enhanced loss can result from $\mathbf{E} \times \mathbf{B}$ drifts arising from fluctuating electric fields. A host of microinstabilities (i.e. instabilities with spatial scales much smaller than the plasma radius) could be invoked as the source of such fluctuations. In addition, many instabilities involve magnetic perturbations which can modify the magnetic field structure. The ideal, nicely nested magnetic surfaces can even be randomized by magnetic field fluctuations, so that energy and particles are lost via flow along the resultant stochastic magnetic field lines. In case the plasma is so strongly excited that a continuous spectrum of frequencies is present, it is in a state of turbulence.

It is perhaps not surprising that no convincing theoretical model has arisen due to this multitude of possibilities for the cause of anomalous transport and the technical difficulties in calculating their consequences. Therefore, dedicated experiments are needed to gain more insight in the physics of plasma fluctuations and transport.

The mechanisms causing the anomalous losses do not appear to be affected by the size of the plasma. Therefore, fundamental research can be carried out in a dedicated medium-sized tokamak without losing relevance for larger devices. The FOM-Instituut voor Plasmafysica 'Rijnhuizen' has dedicated its fusion research programme completely to the study of transport mechanisms in tokamak plasmas. In order to carry out the research, the medium-sized tokamak RTP (Rijnhuizen Tokamak Project) has recently been built with preferential support from Euratom. The experimental work will focus on determining as accurately as

possible the radial and poloidal structure of the plasma equilibrium and of the fluctuation spectra excited in the frequency bands that can be expected to cause turbulent transport of plasma particles and energy. In addition to analysing plasmas with ohmic and intense electron cyclotron heating (ECH: up to 400 kW power at 60 GHz) in steady state conditions, a large effort will be made to study the space-time evolution of relevant plasma parameters for transient states, as a response to well-defined perturbations by local electron cyclotron heating and pellet injection. It should be noted that the ECRH power can be launched from both the low-field and the high-field side. By means of mirrors the launch angle can be varied in toroidal and poloidal direction. This allows to use heating at down-shifted frequencies to generate supra-thermals, and hopefully, current drive. In case of successful current drive, its effect on fluctuations and transport will be studied.

Poloidal dependencies of the plasma state are important to identify the specific toroidal effects on plasma transport as predicted by neoclassical transport theory and generalizations of it which also include anomalous transport phenomena. While simple approximations to neoclassical transport theory cover only small poloidal variations, there are indications that these variations are sizeable in tokamak plasmas and could possibly be directly related with the enhanced losses observed.

The diagnostical programme of RTP will be fully dedicated to the above research themes. This implies that many diagnostics are especially designed to measure one or more plasma parameters with high accuracy and with good spatial and temporal resolution.

I Description of the RTP tokamak

The RTP tokamak, which is a rebuild of the former PETULA tokamak from the EURATOM-CEA association in Grenoble, is presently being commissioned at the FOM-Instituut voor Plasmafysica 'Rijnhuizen'. A cross-sectional view of the machine is shown in Fig. 1. Selected machine and plasma parameters are given in Table I.

Table I: Selected RTP Parameters		
Major radius		0.72 m
Minor radius at limiter		0.16 - 0.185 m
Inner radius of vacuum vessel		0.235 m
Plasma current		200 kA
Loop voltage		1.5 V
Toroidal field		2.6 T
Flux swing		1 Vs
Pulse time		250 ms
MHD safety factor at edge		> 2.2
Electron density :	line averaged	$< 9 \times 10^{19}$ m^{-3}
	central	$< 2 \times 10^{20}$ m^{-3}
Electron temperature:	central (OH)	1 keV
	central (ECH) low density	2.8 keV
	central (ECH) high density	1.3 keV
Ion temperature:	central (OH)	0.6 keV
	central (ECH) low density	0.2 keV
	central (ECH) high density	0.8 keV
Z_{eff}		1.5
Energy confinement time (OH)		10 ms
Energy confinement time (ECH)		3 ms
Ohmic input power		0.3 MW
ECR heating power		0.4 MW

One of the two available 60 GHz, 200 kW gyrotrons for ECRH will be permanently connected to a low-field-side launcher (i.e. outboard) and the second one will be switchable between a low and a high-field-side (i.e. inboard) launcher. The polarization will be controlled by rotation of the TE_{01}-TE_{11} converters present in all three transmission lines.[3]

Inboard launch will be realized by using a top port and reflecting the radiation from a mirror.[4] This set-up allows both outboard or combined outboard/inboard launch to a

maximum of 400 kW or inboard launch with 200 kW. An important tool will be the facility to modulate the output power of individual gyrotrons. This allows studies of the transient response of the plasma to a modulation with variable frequency and amplitude. Statistical analysis of the results from many identical modulations during one pulse improves the signal-to-noise ratio. The heating pulse of 100 ms allows at least 10 repeated modulations on a time-scale comparable to the energy confinement time of RTP.

1 core
2 outer limb
3 coil B_ϕ
4 plasma
5 vacuum vessel
6 coil B_θ
7 coil B_V
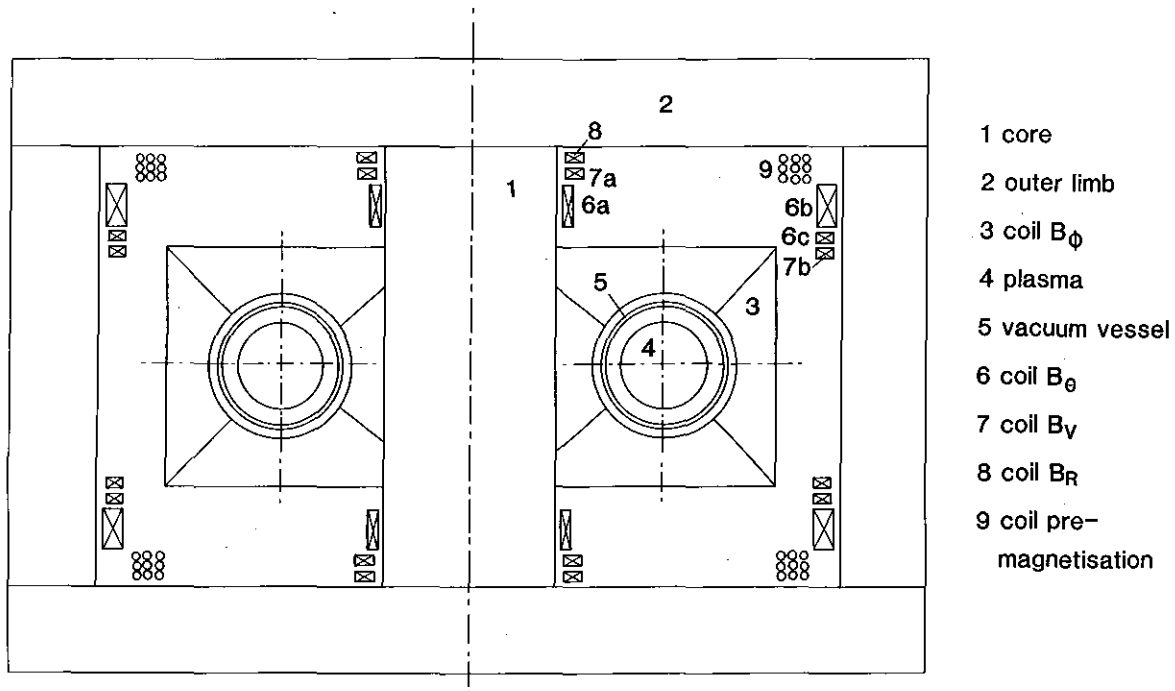8 coil B_R
9 coil pre-
  magnetisation

Fig. 1   Cross-sectional view of the RTP tokamak.

A multiple pellet injector will be available from 1991 onwards, allowing the launching of up to 8 pellets with a diameter of 0.8 mm. The transient response of the plasma to the resulting density and temperature perturbations will reveal the nature of some transport properties.

II   RTP diagnostical programme

The RTP diagnostical programme will focus on two issues: (a) the temporal and two-dimensional spatial determination of plasma quantities with a time resolution related to transport relaxation times, and (b) the investigation of turbulent spectra of various plasma parameters over a wide frequency range. The diagnostics on RTP are subdivided into five separate topic groups according to the employed techniques: 1) machine control diagnostics, 2) laser diagnostics, 3) mm and sub-mm diagnostics, 4) particle diagnostics and 5) spectroscopic diagnostics. The choice for the specific diagnostics in each group was strongly influenced by the available experience and hardware within the institute. Some of the diagnostics have already been employed at earlier experiments at Rijnhuizen, i.e. the TORTUR tokamak[5] and the SPICA II screw-pinch.[6]

Fortunately the diagnostic accessibility of the RTP vacuum chamber is good with numerous ports as shown in the port allocation scheme (Fig. 2). A total of 11 large horizontal ports are present (4 times 360×96 mm^2, 4 times 412×120 mm^2 and 3 times 310×140 mm^2), 8 of them are allocated to diagnostics. The distance from the port window to the plasma edge is approximately 0.55 - 0.6 m, depending on the port. The height of the horizontal ports allows to diagnose the complete minor cross-section of the plasma. Top and bottom vertical ports are located at several toroidal positions. Some of them extend over the complete minor radius of the plasma to facilitate the use of multichord diagnostics. The distance from the port window to the plasma edge is about 0.3 - 0.4 m for the vertical ports, creating some difficulties for diagnostics which must be located near the plasma boundary with regard to stable support and cooling of the diagnostic components.

The RTP diagnostics programme for the next few years is indicated schematically in Fig. 3. In the course of 1989 those diagnostics become available which were already used at the TORTUR and SPICA devices. These diagnostics will mainly measure bulk plasma parameters. At the end of 1989 new and more advanced multichord diagnostics become available, which will be especially dedicated to the measurement of fluctuating quantities with good spatial and temporal resolution. From 1990 onwards new diagnostics will be built and implemented on the machine. However, funding of some of these diagnostics still has to be obtained from additional sources.

In Table II a listing is presented of the techniques used to measure various plasma parameters. The diagnostics will be presented in more detail in the succeeding sections, where they are grouped according to the measuring technique.

Heterodyne ECE

tangential X-ray PHA

X-ray + visible light tomography

collective scattering interferometry polarimetry

ECRH diagnostics

gaspuf + 4 fast coils

ion source

ECRH

2 - mm interferometry

bolometry

ECRH

4 fast coils

4 fast coils

inside

top

outside

bottom

inside

diamagnetic loop

24 slow coils

movable limiter + pellet injector

Rutherford scattering

4 fast coils

reflectometry

tangential Thomson scattering

VUV - spectrometer

ECE polychromator + limiter

ECRH diagnostics

neutral particle analyser + CXRS

collective scattering interferometry polarimetry

Thomson scattering (laser in + profile measurement)

toroidal coil number   1   2   3   4   5   6   7   8   9   10   11   12   13   14   15   16   17   18   19   20   21   22   23   24   1
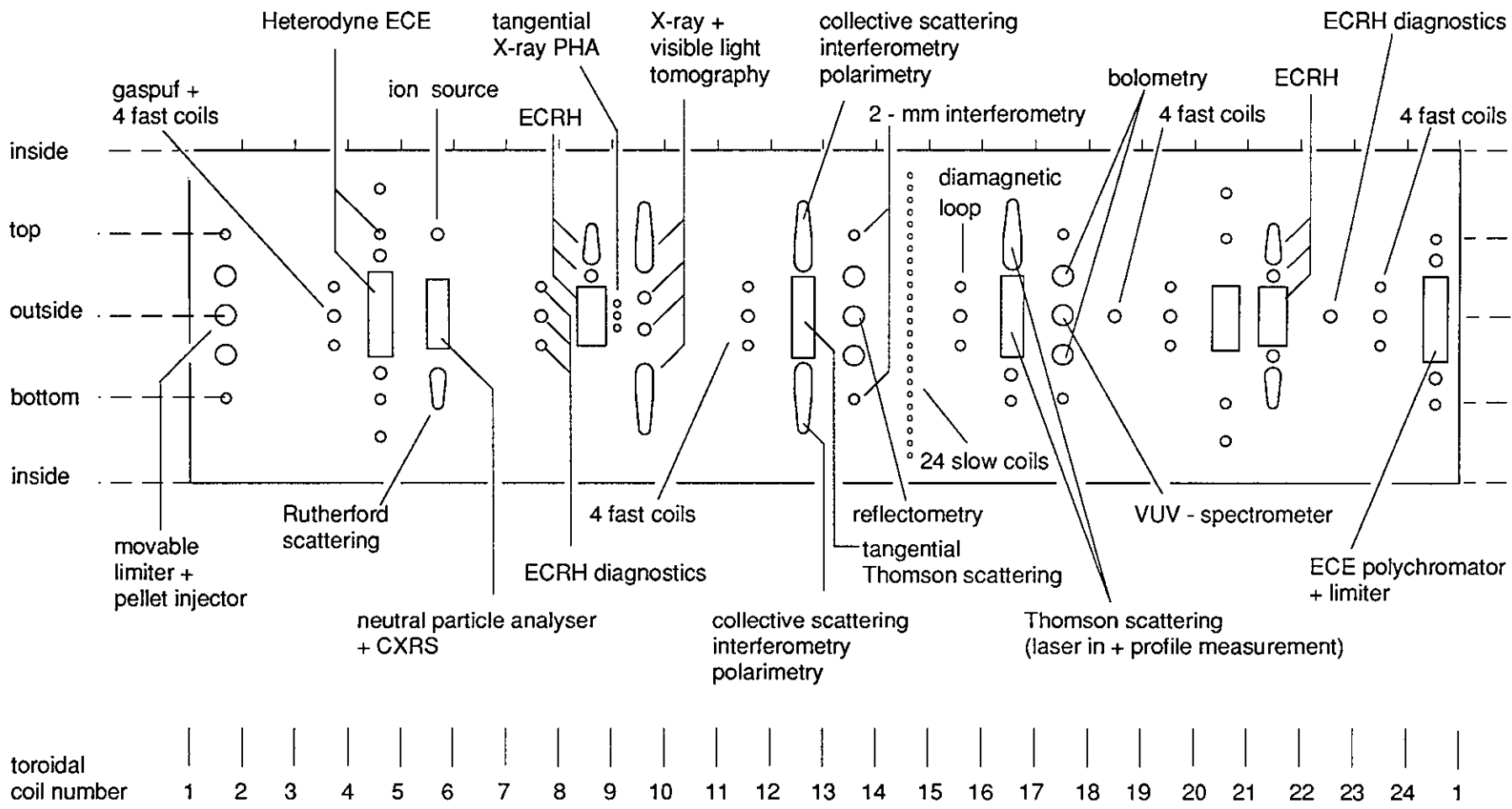
Fig. 2   *Port allocation of the various diagnostics.*

The horizontal axis (length 2πR) refers to the toroidal location and the vertical axis (length 2πa) to the poloidal location.
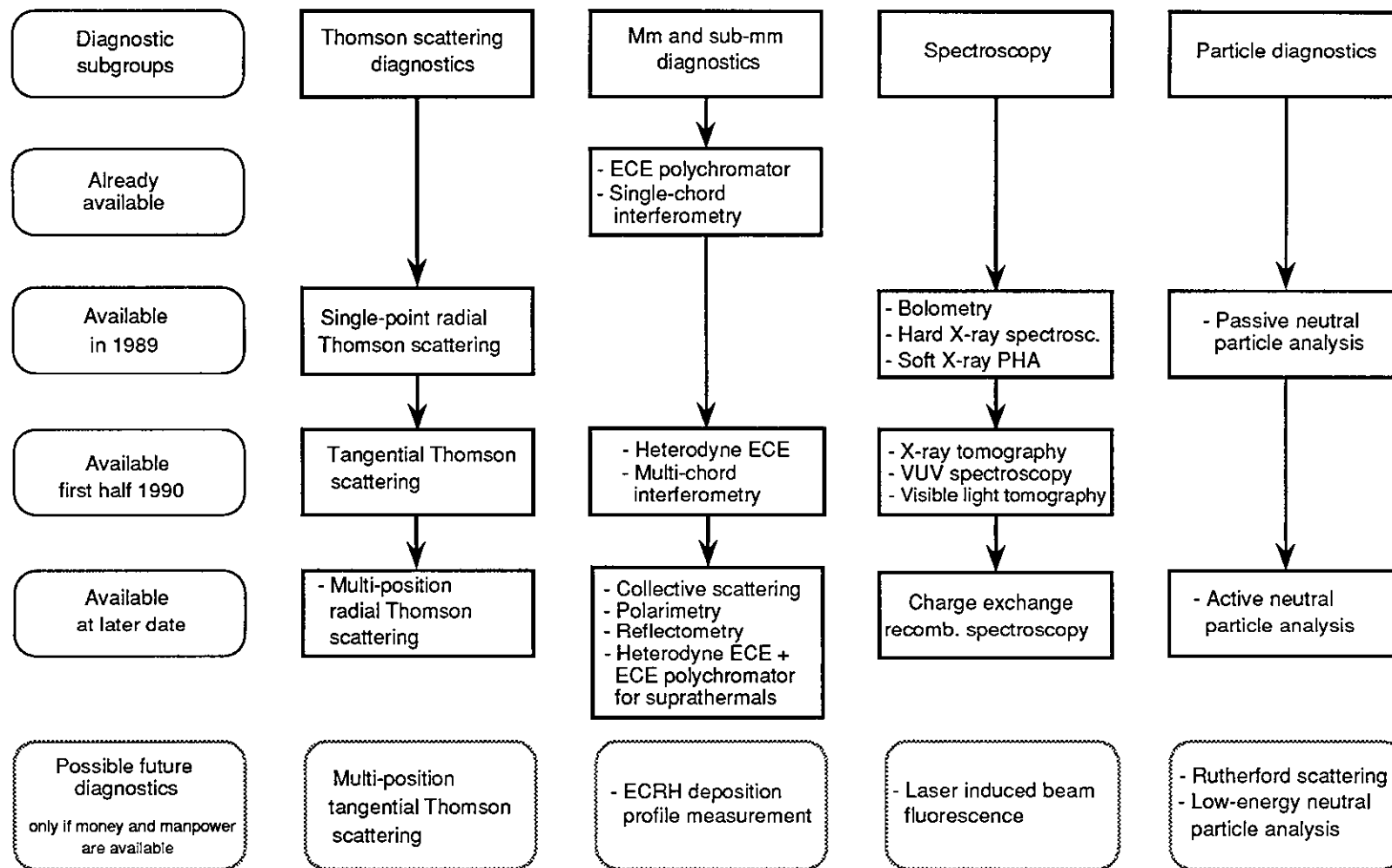
Diagnostic subgroups	Thomson scattering diagnostics	Mm and sub-mm diagnostics	Spectroscopy	Particle diagnostics
Already available		- ECE polychromator - Single-chord interferometry		
Available in 1989	Single-point radial Thomson scattering		- Bolometry - Hard X-ray spectrosc. - Soft X-ray PHA	- Passive neutral particle analysis
Available first half 1990	Tangential Thomson scattering	- Heterodyne ECE - Multi-chord interferometry	- X-ray tomography - VUV spectroscopy - Visible light tomography	
Available at later date	- Multi-position radial Thomson scattering	- Collective scattering - Polarimetry - Reflectometry - Heterodyne ECE + ECE polychromator for suprathermals	Charge exchange recomb. spectroscopy	- Active neutral particle analysis
Possible future diagnostics only if money and manpower are available	Multi-position tangential Thomson scattering	- ECRH deposition profile measurement	- Laser induced beam fluorescence	- Rutherford scattering - Low-energy neutral particle analysis

Fig. 3   Overview of the RTP diagnostical programme.

Table II: RTP Preliminary Diagnostic List
(printed in italic: expertise and designs are available, but funding still has to be found)

Electron density

　　Single-point radial Thomson scattering

　　20-channel radial Thomson scattering (to measure a vertical profile)

　　20-channel tangential Thomson scattering (to measure a vertical profile)

　　Single-chord 2-mm interferometer (for density feedback)

　　Max. 19-chord 400 μm interferometer (measuring vertical line-integrated densities)

　　3-channel reflectometer (in- and outboard antennae); *to be extended to 12 channels*

Electron temperature

　　Thomson scattering (see electron density)

　　6-channel electron cyclotron emission (grating polychromator)

　　20-channel heterodyne electron cyclotron emission radiometer

　　X-ray pulse height analysis (along a tangential chord)

Ion temperature

　　Neutral particle analysis (passive and active)

　　Charge exchange recombination spectroscopy (H or He diagnostic beam)

　　Small-angle Rutherford scattering

Emission of radiation

　　80-channel visible light tomography

　　80-channel X-ray tomography (5 cameras of 16 channels each)

　　Bolometry

　　X-ray pulse height analysis

　　VUV and XUV spectroscopy

Magnetic properties

　　Rogowski loop

　　2 Flux/voltage loops (outside and inside)

　　2 sets of 24 (12 radial and 12 poloidal) pick-up coils in a poloidal annular tube

　　4 sets of 4 toroidal pick-up coils

　　Diamagnetic loops

　　12 Saddle loops

Current density

    Tangential Thomson scattering (see electron density)

    10-chord 400 μm polarimeter (vertically injected beams)

Wave activity

    Mirnov loops (poloidal and toroidal arrays inside the vacuum vessel)

    20-channel heterodyne electron cyclotron emission radiometer

    80-channel X-ray tomography

    80-channel visible light tomography

    3-channel reflectometry; *to be extended to 12 channels*

    7-channel collective FIR scattering

ECRH wave-plasma interaction

    FIR or IR collective scattering

Edge/divertor phenomena

    H_α-monitors

    80-channel visible light tomography

    Low-energy neutral particle analysis (10 - 200 eV)

Suprathermal electron distributions

    6-channel grating polychromator for electron cyclotron emission

    20-channel heterodyne ECE radiometer (equipped with top and inboard antennae)

    4-channel Thomson-scattering polychromator tuned to tail populations

    X-ray pulse height analysis

III   <u>Description of the diagnostics in the various topic groups</u>

In this chapter a description will be given of the various diagnostics which are envisaged for the RTP tokamak. It is not possible to give a complete description of all the diagnostics, mainly for two reasons. Firstly, this report would become too long if we would go into detail for every diagnostic. Secondly, some diagnostics are still in the design phase so that particular instrumental and physical aspects are subject to changes.

For the various diagnostics we will present the arguments for implementing it on RTP, the physical information we hope to gain with it as well as the general design philosophy of the instrumental apparatus.

III.1   Machine diagnostics

Since the instrumentation in this group is closely related to machine operations, the design and construction is done by the operations staff. Here only a short description will be given of the main systems.

Highly reproducible RTP discharges can be obtained by a sophisticated feedback system, controlling the plasma current and position. An accurate setting of the initial vertical and radial field strengths is necessary to obtain breakdown. The plasma current and position are measured by means of two sets of 24 small pick-up coils inside annular stainless steel tubes fixed on the inner toroidal surface of the vacuum chamber. The values of the plasma current and its position are then calculated by fast digital algorithms and after DA-conversion fed back to the thyristor control modules of the poloidal coil power system. For the feedback control only one of the two sets of poloidal pick-up coils is used, the other one will be used to measure magnetic field fluctuations with frequencies up to several tens of kHz. A Rogowski coil mounted on the outside of the vacuum chamber will measure the sum of the plasma current and the current through the liner. Comparison with results from the pick-up coils will yield the ratio of plasma to liner resistance. A third set of 24 pick-up coils will be mounted in a ceramic tube to facilitate field fluctuation measurements at frequencies up to several hundreds of kHz. Supplementary pick-up coils will be mounted at several toroidal positions to measure the toroidal correlation length of the magnetic field fluctuations. Twelve partial saddle loops at various toroidal and poloidal locations are used to measure the vertical and horizontal magnetic fields on the liner.

The plasma density will be controlled by a feedback system consisting of a single-chord 2 mm interferometer and piezoelectric dosing valves. The beam of the interferometer is injected vertically through the centre of the plasma. A varactor-tuned Gunn oscillator with tripler (output power 10 mW), oversized 30 mm waveguide and quartz Brewster windows will be used. The measured losses and reflections of the Brewster windows are less than 1%. The open end of the 30 mm waveguide gives a good antenna profile. The interferometer will be equipped with two data-acquisition systems. One system has an accuracy of 1/16 of a fringe

and has a sample time of 1 ms. This system will be used for density control. The other system has an accuracy of 1/64 of a fringe and has a sample time of 10 μs. This system will be used for diagnostical purposes.

Hard X-ray monitors will be mounted close to the limiter to measure the integrated flux of hard X-rays during each shot, to ensure the HXR level is environmentally acceptable. A separate hard X-ray monitor will be used for diagnostical purposes (see section III.5). A residual gas analysis system is used to monitor the gas discharge cleaning process.

III.2   Laser diagnostics

Thomson scattering was chosen on RTP since it has some obvious advantages over other diagnostics:

- localized and absolute measurements of the electron temperature and density can be performed with high accuracy ($\approx$ 1% at T_e = 1 keV and n_e = 5 × 10^{19} m^{-3}).
- These measurements can be performed either at a single-point or at various points (20-40) along the laser chord (unfortunately, at only one instant during the discharge).
- by means of a tangential viewing option it is also possible to deduce the local current density in the centre of the plasma directly from the shift of the complete scattering distribution with about 10% accuracy (see Section III.2.3).
- Thomson scattering can be used for absolute calibration of other diagnostics (e.g. electron cyclotron emission) for which direct calibration methods are not as definitive.

A 10 joule Q-switched ruby laser (λ = 694.3 nm) will be used for all Thomson-scattering diagnostics at RTP. The laser beam, which has a 20 ns pulse duration, will be injected vertically through the centre of the plasma. First Thomson-scattering observations will be done by means of a single-point system. In a later stage a multiposition system will be added for simultaneous measurements at 20 positions along the laser chord. Both systems will observe the light scattered over about 90° in the radial direction. A subsequent extension of the system will be an additional detection branch observing the laser beam from the tangential direction. This will enable direct measurements of the local current density distribution in the RTP plasma. Many components of the Thomson-scattering system were already in use or tested on the TORTUR tokamak.[7,8] Hence, most of the hardware is already available. Beside measurement of the electron temperatures and densities at one time-instant, the Thomson-scattering diagnostic will be important for absolute calibration of the various ECE diagnostics.

III.2.1   Single-point Thomson scattering

Light from a 15 mm high volume scattered over 90° in a solid angle of 10 msr will be collected by a twenty-channel 45% transmission polychromator[8,9] using photomultipliers equipped with GaAs photocathodes (see Fig. 4). The high transmission will be achieved by using mirrors instead of fibre optics to guide the spectrally resolved light to a set of photomultipliers. Spectral analysis is performed with a holographically ruled concave grating. Acceptable dimensions of the wavelength selection mirrors were obtained by magnifying the spectral image by a factor of 5 with a Mangin mirror. Both the red and the blue wings of the scattered spectrum will be observed. The twenty channels cover a spectral range from 600 to 800 nm, which allows the detection of electron temperatures from 5 eV to 2 keV. This large dynamic range could be realized by using different spectral bandwidths for the various channels (4.5 nm close to the laser beam and 13 nm at the edge of the spectrum). Background light will be measured just before and after the laser pulse. T_e- and n_e-measurements can be performed with 1% accuracy at $n_e = 5 \times 10^{19}$ m^{-3}. In Fig. 5, a typical spectrum, as measured before with the twenty-channel polychromator (on the TORTUR tokamak) is shown.

At the TORTUR tokamak strong distortions in the electron-velocity distribution were observed with the twenty-channel polychromator[5,10] (see Fig. 5). The distortions were present on both wings of the scattering distribution. The magnitude of the distortions appeared to be much larger in the tangential direction than in the radial direction. The partial electron density responsible for the satellites was typically $0.5 - 1 \times 10^{18}$ m^{-3}, which is about 1 - 2% of the total number density. Similar deviations from a maxwellian distribution have been observed also on other devices.[11-14] Special attention will be devoted to see whether satellites are also present in the RTP plasma or not. If they are, a systematic study will be undertaken to understand the cause of these distortions.
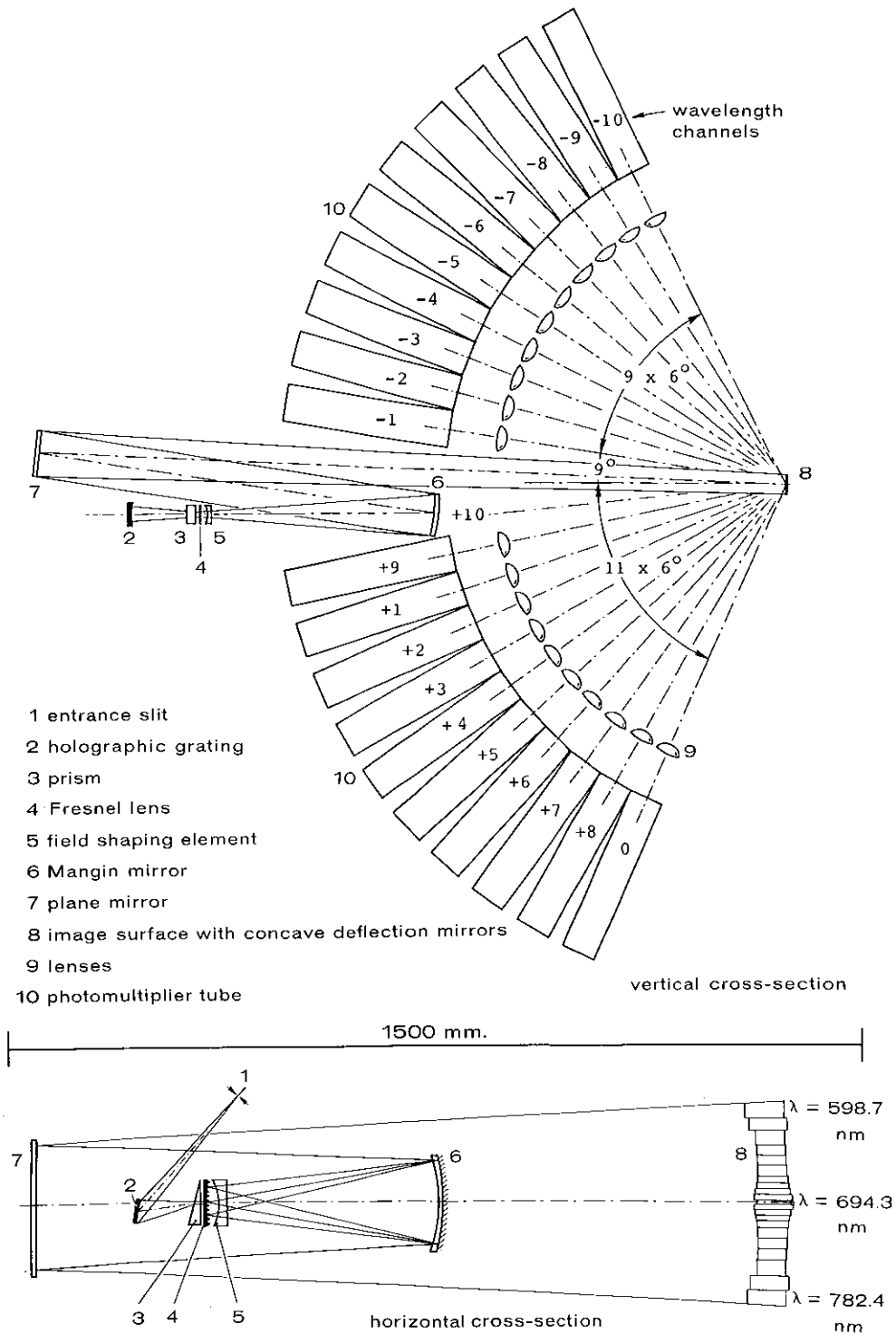
14

wavelength
channels

1 entrance slit
2 holographic grating
3 prism
4 Fresnel lens
5 field shaping element
6 Mangin mirror
7 plane mirror
8 image surface with concave deflection mirrors
9 lenses
10 photomultiplier tube

vertical cross-section

1500 mm.

λ = 598.7 nm

λ = 694.3 nm

λ = 782.4 nm

horizontal cross-section

Fig. 4 *Vertical and horizontal cross-sections of the 20-channel polychromator. After dispersion by the grating (2), the intermediate image of the spectrum is formed between (3) and (4). This image is magnified five times by means of a Mangin mirror (6). Twenty-one concave mirrors (8) each deflect a small spectral range into the photomultiplier.*
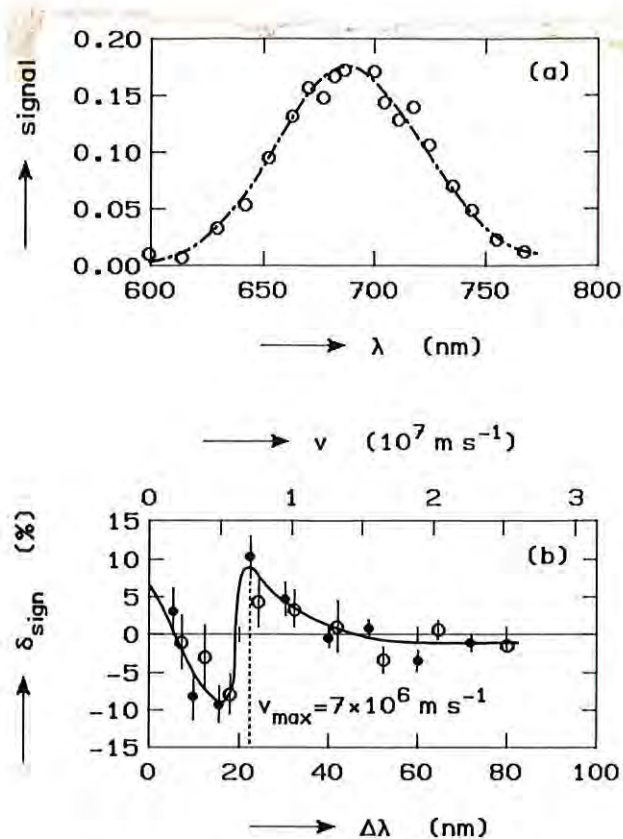
Fig. 5   *(a) Thomson-scattering spectrum ($T_e = 594 \pm 8$ eV and $n_e = (5.57 \pm 0.08) \times 10^{19}$ m^{-3}). The dashed line is a relativistic gaussian fit to the data. (b) Deviations of the data from the gaussian. The open circles correspond to the blue wing and the filled circles to the red wing of the spectrum. $\Delta signal = [y - y (fit)]/A$, where A is the amplitude of the gaussian and y is the signal.*

III.2.2   Multipoint Thomson scattering

The optical system to perform profile measurements by means of Thomson scattering along the vertical laser chord has been tested also at the TORTUR tokamak.[7,15] Similarly to the single-point system the transport of the light from the tokamak to the polychromator is done by means of conventional optics instead of fibre optics. The scattered light (see Fig. 6) is collected by a triplet lens (item 3) and guided to a Littrow polychromator by means of several mirrors and a f = 1.7 m achromatic doublet. The spherical mirrors (items 4, 10 and 13) serve for pupil imaging and field curvature correction. The flat mirrors are brought in to fold the optical path. One spherical mirror (item 10) serves as entrance "slit" of the polychromator. The grating (item 12) is tilted in such a way that the central wavelength of the ruby laser returns along the optical axis. In this way the vessel stray light is filtered out. The spectrum is collected by means of mirror number 13 and imaged on to the detector surface with a f = 25 mm high speed (f/0.95) camera objective. The detector consists of a microchannel plate intensifier coupled with a fibre optic face plate to a charge coupled device.
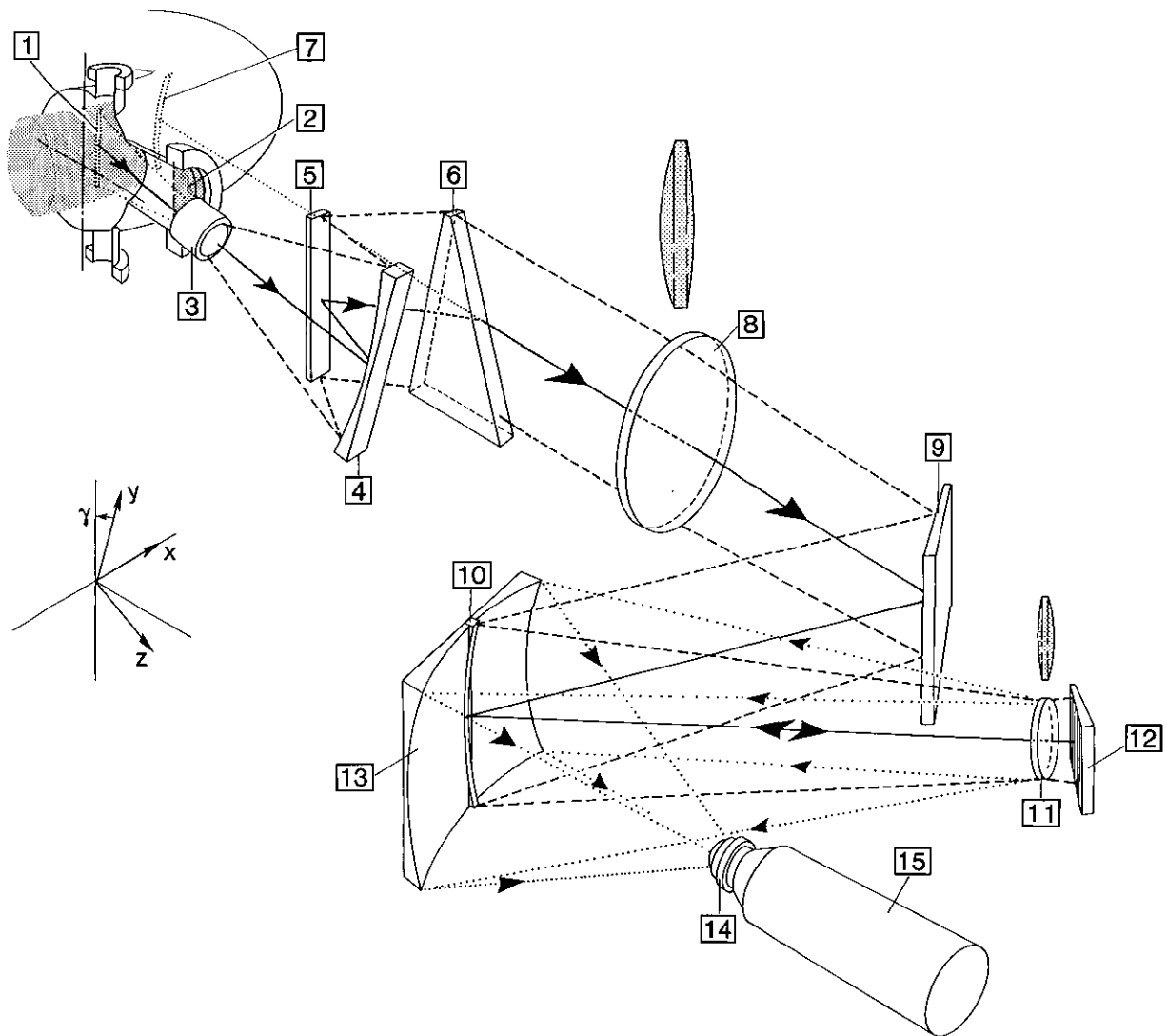
Fig. 6   Schematic drawing for multiposition Thomson scattering: (1) laser beam, (2) vacuum window, (3) triplet lens, (4) concave mirror, (5) plane mirror, (6) prism, (7) image of the laser beam as seen by (8) doublet lens, (9) plane mirror, (10) spectrometer input mirror, (11) spectrometer lens, (12) grating (600 ll/mm), (13) concave mirror, (14) detector lens and (15) television camera.

The quality of the optical system was tested on a test bench and was found to confirm the design values very well. The total system was implemented on the TORTUR tokamak, but no Thomson-scattering measurements could be performed due to the high level of vessel stray light and due to the short measuring period left before the TORTUR device was disassembled.

The multiposition Thomson scattering device will enable measurement of the vertical electron temperature and -density profiles along the laser chord at one instant. The diagnostic will become available early 1990. It will not make the single-point measurement superfluous, since the twenty-channel polychromator can measure the electron temperature and -density with higher precision.

III.2.3   Tangential Thomson scattering

Usually the wave vectors of the incident and scattered waves are both in a poloidal plane. When the light is observed in the tangential (=toroidal) direction, however, the scattering vector makes an angle of 45° with respect to the plasma current. Since the component of the electron drift velocity, v_d, parallel to the scattering vector gives rise to a measurable shift of the total (tangential) scattering distribution, it becomes possible to determine the local current density $j_\phi = e\, n_e\, v_d$. From the latter value the poloidal magnetic field may be deduced. A proof-of-principle of this method was already given on TTF2,[16] albeit with limited accuracy. Subsequent experiments were carried out at the TORTUR tokamak.[10] Although feasibility studies indicated that the current density may be obtained with an accuracy of approximately 10%,[17] tangential Thomson scattering is not applied at present tokamaks for two reasons. Firstly, the toroidal field coils drastically limit the access to a tangential viewing port. Secondly, the drift velocity causes only a small shift, $\Delta\lambda_d$, of the observed spectrum as compared to its width, $\Delta\lambda_e$. At RTP, however, the possibility exists to view the laser chord from the tangential direction by means of a set of mirrors in one of the large horizontal ports (see Fig. 7). The accuracy of the 20-channel polychromator ($\Delta\lambda = 0.28$ nm) is good enough to measure the local current density in a single laser shot with high precision. In addition measurements of the local current density at the edge are possible, but here one has to take the trapped electron populations into account.

A first attempt to measure the electron drift velocity in one single laser shot was made at the TORTUR tokamak, using ≈ 3.5 J in the scattering volume.[10] Figure 8 shows an example of a single-shot v_d-measurement, from which the following values were obtained: $\Delta\lambda_d = -2.5 \pm 0.5$ nm, resulting in $v_d = 1.1 \times 10^6$ m/s and $j_\phi = 1.0 \times 10^7$ A/m² at $n_e = (5.87 \pm 0.16) \times 10^{19}$ m⁻³ and $T_e = (446 \pm 11)$ eV. The sign of the wavelength shift corresponds to the actual current direction. The current density obtained from T_e and $V_{loop} = 5$ V, assuming Spitzer resistivity and $Z_{eff} = 2$, is 8.3×10^6 A/m², corresponding to $q_0 = 1.2$.
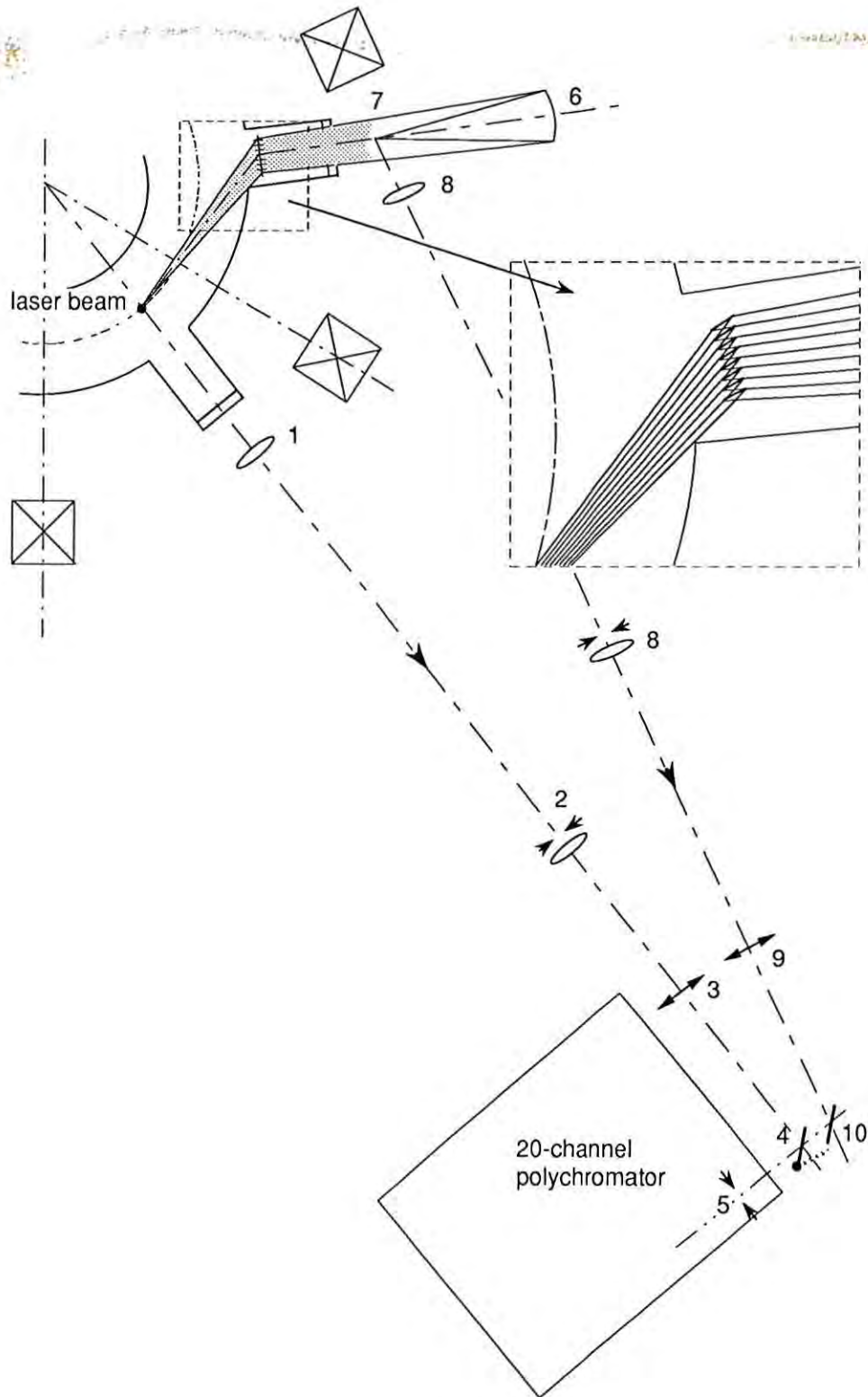
Fig. 7   Geometrical set-up of the tangential Thomson-scattering measurements at RTP.

At higher temperatures (≥ 500 eV) the interpretation of the scattered TORTUR spectra became too difficult because of the earlier mentioned non-thermal features. At these temperatures the deduced current density values became irreproducible.
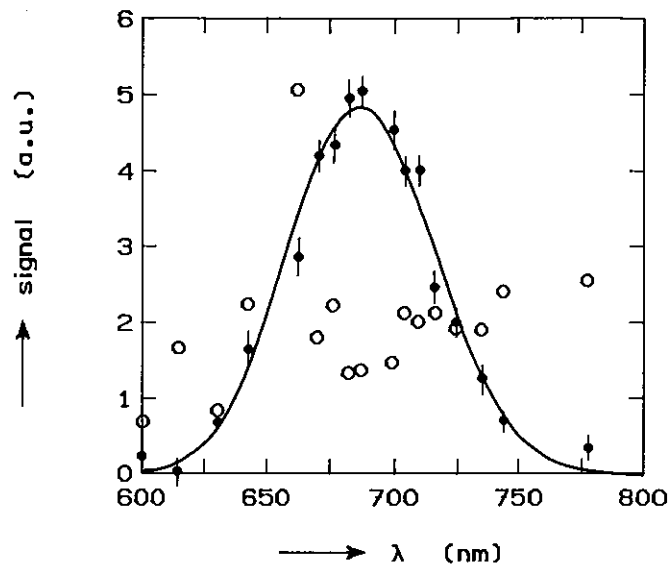
Fig. 8   *Example of a single-shot tangential Thomson-scattering spectrum from which the local current density could be deduced.*

III.3 Millimeter- and submillimeter-wave diagnostics

Since the beginning of fusion research, plasma diagnostic techniques involving various kinds of electromagnetic radiation either from external sources or from the plasma itself have been developed and successfully utilized in many different types of plasma devices.[18] Due to the highly dispersive nature of magnetized plasmas, characteristics of the electromagnetic radiation which was emitted from, transmitted through, reflected from, or scattered by the plasma, will sensitively reflect the properties of the plasma with which it has interacted. The characteristics of the electromagnetic radiation employed in such a diagnostic, such as the frequency, depend on the plasma property to be investigated. For typical present-day tokamak plasmas as in RTP, the appropriate frequency for many diagnostic applications falls within the microwave and far-infrared (FIR) range, with wavelengths in the mm and sub-mm region. In the following, three categories of this diagnostic technique will be described as envisaged for RTP. These are: microwave emission from the plasma (electron cyclotron emission, or ECE), transmission and/or reflection of external electromagnetic waves (interferometer, polarimeter, reflectometer), and scattering by the plasma (far-infrared and infrared collective scattering).

III.3.1   Electron cyclotron emission diagnostic

The electron temperature profile $T_e(r)$ in RTP will be deduced from a measurement of the spectral intensity of the electron cyclotron emission (ECE) at the optically thick harmonics.[19,20] This diagnostic was chosen because it yields the real-time history of relative electron temperature profiles with reasonable spatial resolution ($\approx$ 15 mm in the radial direction) and with fast time response (1 - 5 μs). Unfortunately, direct and accurate calibration of ECE has not become a straightforward procedure yet. Therefore, ECE has to be cross-calibrated against Thomson scattering.

On RTP, two diagnostic techniques will be employed for measurement of ECE: a grating polychromator and a heterodyne radiometer. The two diagnostics are different mainly in the way by which each separates different frequencies or wavelength components (and thus position dependence) in the radiation power collected by the antenna.

III.3.1.1   Grating polychromator

Here, a grating is employed to separate the received ECE radiation into six different wavelength components (see Fig. 9).[21] The spectrally resolved radiation is imaged onto six correspondingly arranged exit wave guides, each of them relaying a part of the radiation spectrum to a liquid-He cooled InSb detector, followed by electronic circuitry and data-acquisition hardware. The 6-channel grating polychromator envisaged for RTP has been used successfully on the TORTUR[22] and T-10 (Moscow)[23] tokamaks. A similar 12-channel polychromator was built for JET[24] and was used to determine the propagation of heat pulses in the JET plasma, induced by sawtooth collapses.[25] The temperature resolution of the grating polychromator at RTP will be about 20 eV. The radial and temporal resolution of the instrument are 15 mm and 5 μs, respectively.

III.3.1.2   Heterodyne radiometer

A heterodyne radiofrequency communication technique is utilized here for spectral resolution.[26] In this technique, one employs a local oscillator (LO) of an exactly known frequency. The output radiation of this LO is combined with the incoming signal radiation on a detector to produce a beat signal at the difference frequency. Typically the detector has a passband for the beat signal (or Intermediate Frequency (IF) signal) defined around the LO frequency. This IF passband in principle determines the frequency resolution. For RTP, the actual ECE receiver configuration is more complicated (see Fig. 10). In this configuration, the LO and the mixer are combined into one unit, a downconverter. The signal from the plasma is split into five branches, and each is fed onto a downconverter (LO frequencies: 80, 92, 104,
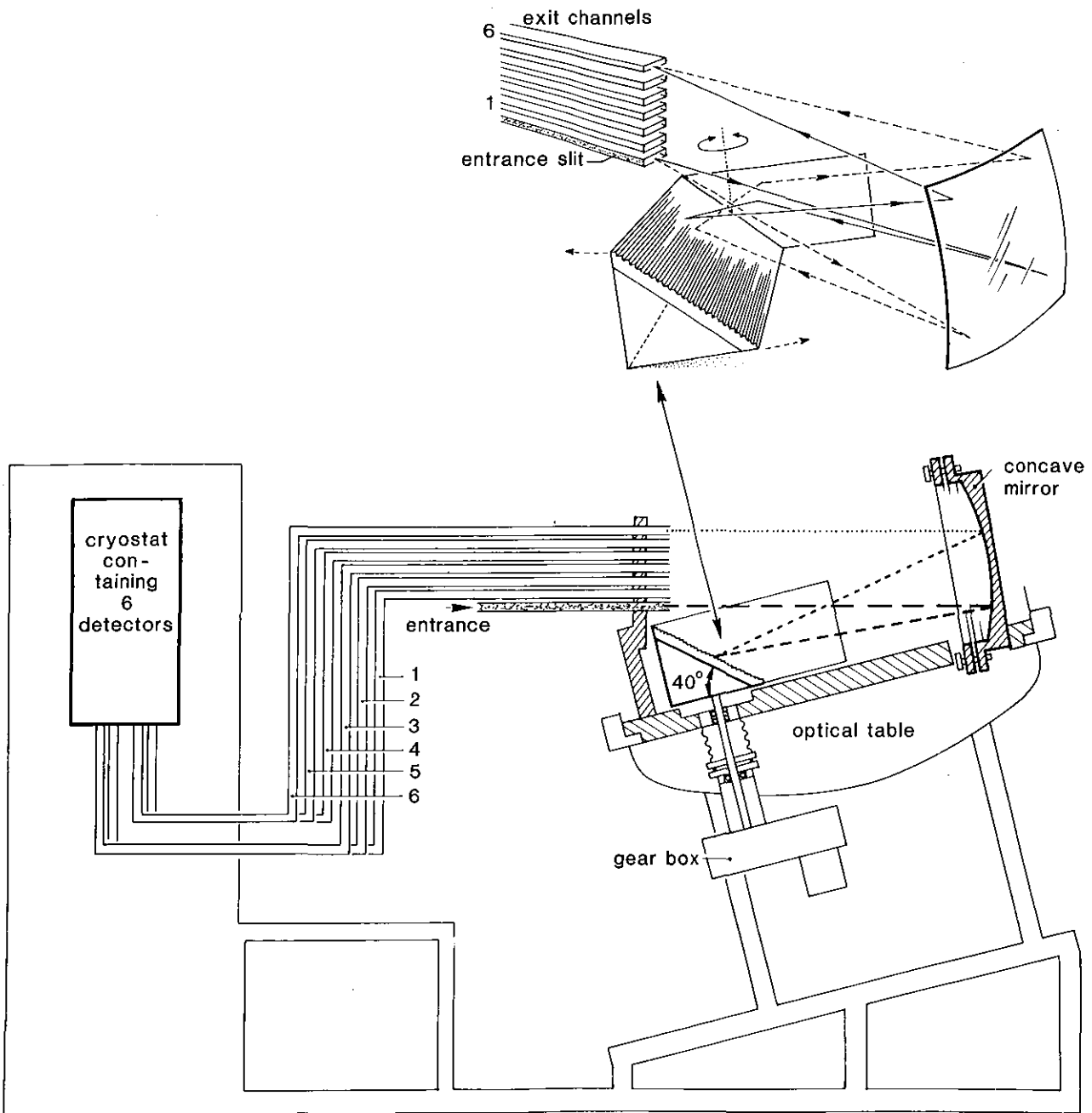
Fig. 9   *Schematic drawing of the 6-channel polychromator for measurement of electron cyclotron emission from RTP.*

116 and 128 GHz, IF band: 6 - 18 GHz). Hence, the outputs of the various downconverters have frequency components in the 6 - 18 GHz range, but they represent different spectral components in the original input ECE radiation. The signals are further decomposed in frequency by applying the same technique: a second set of four mixers, with LOs at 7.5, 10.5, 13.5 and 16.5 GHz and IF bandwidth of 1 GHz, is applied to each of the five downconverters
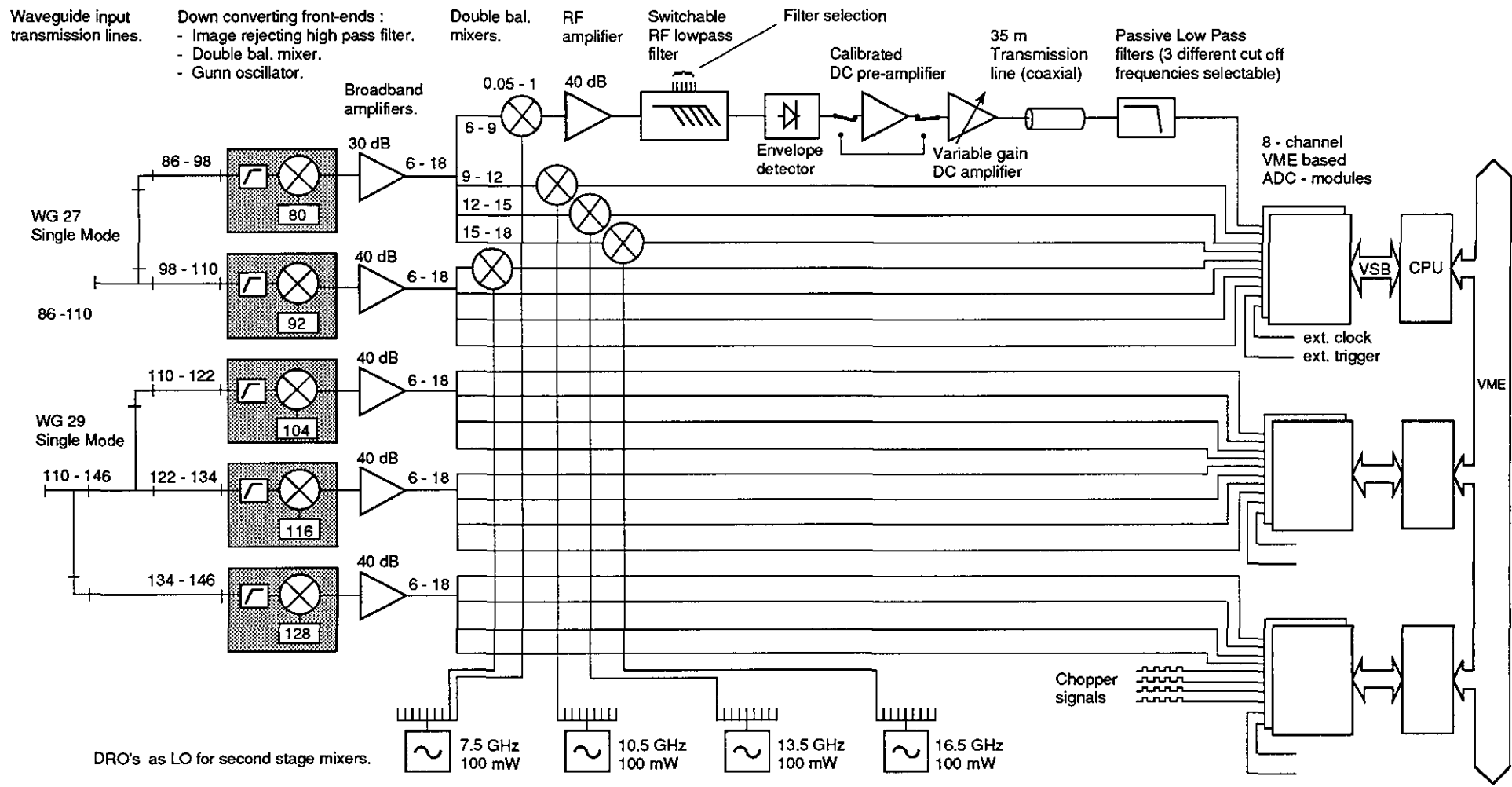
Fig. 10   Schematic overview of the 20 - channel double heterodyne radiometer
(Dimensionless numbers are selected frequency bands in GHz)

of the first set. Overall, therefore, we have 5 x 4 = 20 observation windows of 1 GHz width, covering the range from 85 to 145 GHz, roughly at every 3 GHz, enabling temperature measurements along the entire cross-section of RTP plasma, as long as the central field does not rise above 2 T. Finally, twenty Schottky diode rectifiers will generate a continuous signal of the ECE intensity (i.e. temperature) of each spectral component (corresponding to a certain position inside the plasma). In addition, two independent calibration schemes using a noise source and a blackbody at a known temperature will be used regularly for an accurate determination of T_e. The expected temperature resolution is better than 1 eV for a temporal resolution of 10 μs. The maximum temporal resolution is 1 μs. The spatial resolution will be 5 - 20 mm depending on position.

Beside two antennae mounted at the low-field side in the equatorial plane (at one toroidal location), additional antennae will be mounted at the high-field side and in a top port. This will be especially useful for diagnosing highly non-thermal electron distributions.[27] From the top port the plasma is viewed along a line of constant magnetic field. In such a situation there is a simple one-to-one relationship between frequency and total (relativistic) electron energy, provided harmonic overlap is negligible. As a result, one will be able to diagnose the chord-averaged number density and velocity anisotropy of electrons as a function of energy. At RTP special attention will be devoted to the study of collisionless diffusion of suprathermal electrons generated by applying ECR heating from the high-field side in slide-away discharges.

III.3.2   Transmission and reflection diagnostics

III.3.2.1   Interferometer

For frequencies much higher than any plasma characteristic frequencies such as the cyclotron frequency (~ 60 GHz for RTP) or the plasma frequency (< 100 GHz), the plasma dispersion is much simplified and independent of the polarization of the electromagnetic radiation with respect to the magnetic field as far as it is propagating perpendicular to the field. By comparing the relative phases, ϕ, of two waves, one transmitted through vacuum and the other through the plasma, one can obtain information on the plasma density integrated along the line-of-sight.[28] Therefore, a multichannel system is needed to obtain a profile of phase shift ϕ, which is then to be Abel-inverted to get the density profile $n_e(r)$.

On RTP a 19-channel (max.) FIR interferometer is under construction[28] (see Fig. 11). Here a heterodyne technique is employed to achieve interferometry as a phase measurement of the IF signal rather than as an amplitude measurement resulting from direct homodyning. Probe and local oscillator are provided by a twin-frequency FIR laser, whose output frequencies are separated by ~ 1 MHz. Both the LO and the probe beams are expanded in one dimension to simplify the optical arrangement. The width of the slab-like probe beam covers almost the complete poloidal cross-section of the RTP plasma. After passage through the

plasma, the probe beam is combined with the reference beam onto the detectors which are configured in a linear array (see Fig. 12). The detectors each consist of a Schottky-diode corner-cube mixer and a parabolic mirror, for high sensitivity and time response. The detectors can be positioned individually along the linear rail structure. In this way a higher number of detectors can be used for those regions of plasma where the most interesting (density) features are to be expected. It is expected that the phase resolution of the interferometer will be in the $10^{16}\,\mathrm{m}^{-3}$ range. This will permit detailed measurements of small-scale density phenomena such as sawteeth and internal MHD oscillations.
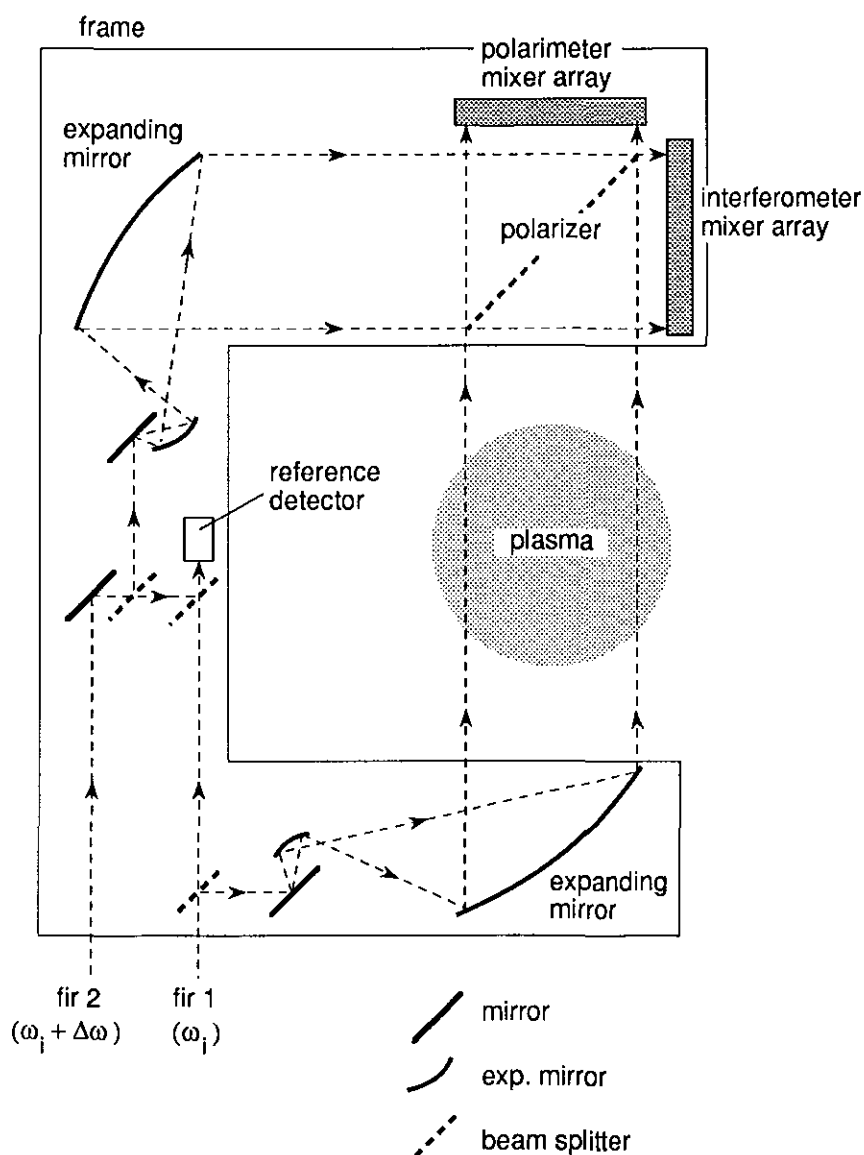
Fig. 11   *Schematic lay-out of the multichannel interferometer/polarimeter to be used at RTP. The detector arrays consist of 10 - 19 individual mirror/mixer units, mounted on linear rail structures. In first instance only one array is used for interferometry. In this case a beam combiner will be used instead of a polarizer.*

Fig. 12   Photograph of one of the detector arrays, showing clearly the individual mixer/mirror combinations which can be shifted along the rail structure.

III.3.2.2   Polarimeter

The multichannel interferometer on RTP will be extended to a multichannel polarimeter (see Fig. 11). The principle of operation of this interferometer/polarimeter is similar to that of Soltwisch,[29] where the polarization component which is normal to the original as a result of the Faraday rotation effect is separated out by a polarizing wire grid. The transmitting part of the FIR power gives the interferometer signal. A maximum of 10 channels each on the interferometer and the polarimeter along with high sensitivity Schottky-diode mixer detectors will produce profiles of the Faraday rotation angle with a resolution of ~ 0.1°. This Faraday rotation profile data provides information about the plasma current density profile and thus the MHD stability of the plasma.

III.3.2.3 Reflectometer

Usually measurements of the electron density profile with an interferometer are very reliable and (depending on the fringe counters used) also rather fast. However, an obvious shortcoming of this diagnostic is the necessity for Abel-inversion techniques to obtain local densities. The actual density distribution often shows a strong departure from cylindrical geometry, which can change on a fast timescale. For instance the (LIDAR) Thomson-scattering results at JET reveal that the standard Abel inversion of the multichannel interferometer data often gives inaccurate local density values.[30]

Therefore, at RTP a 12-channel reflectometer will be used to provide a continuous density measurement with a fast time resolution without making use of inversion or tomographic techniques. Initially 3 channels will be used, to be extended to 12 if funds can be found. Of course, a disadvantage of reflectometers is that they cannot measure inside a hollow electron density profile. Therefore, much interesting information is expected to be obtained from a correlation of the reflectometer and interferometer diagnostics. The reflectometer for RTP will be built by making use of the experience gained in the design construction and operation of a 12-channel reflectometer for JET.[31,32] The principle of a 3-channel reflectometer in the Ka-band (27 - 40 GHz) is shown in Fig. 13. The specifications of the reflectometer are given in Table III.

In the proposed system three waves with frequencies of 27015, 33020 and 39025 MHz, respectively, are launched into the plasma from both the high- and the low-field side. One local oscillator (LO) at 3 GHz is used for the three reflectometer channels. The properties of the harmonic mixers are such that their output signal contains, amongst other combinations, also the difference between the n-th harmonics of the local oscillator and the incoming signal, e.g. 27000 MHz and the incoming 27015 MHz. The 33 and 39 GHz channels will behave similarly. By using different frequency off-sets for the three varactor-tuned Gunn oscillators, the three intermediate frequency (IF) signals at 15, 20 and 25 MHz, respectively, can be separated with band-pass filters. False mixing products due to intermodulation effects are rejected by the band-pass filters. The three IF signals are separately downconverted to one common frequency appropriate for the phase detector. The single fringe output of the phase detector will be recorded with a new VME data-acquisition system with an internal microprocessor (see Section IV), giving us the possibility to change the fringe counter system to our own convenience. Compared to the JET reflectometer, where each channel consisted of two Gunn oscillators and two fundamental mixers, the new design is a factor 3 less expensive. The use of harmonic mixers, with ~25 dB conversion loss, was not possible in the JET reflectometer because of the high overall waveguide (~60 m long) losses.
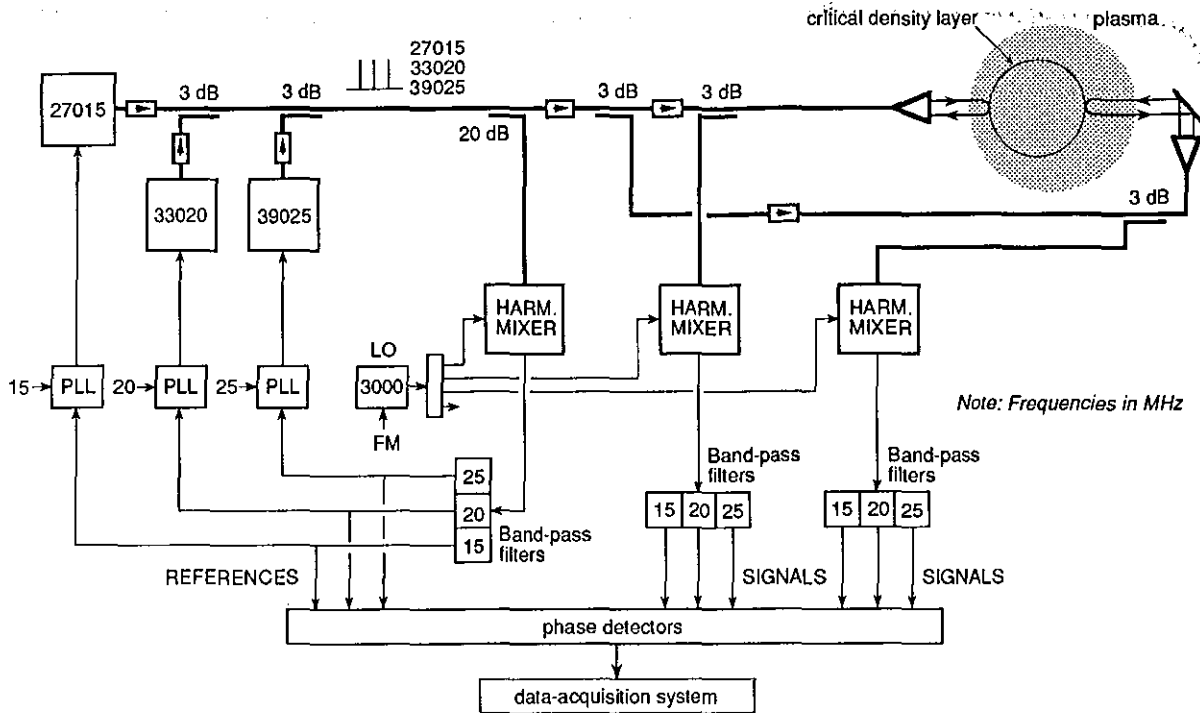
high- and low-field side 3-channel Ka-band reflectometer

Fig. 13 *Scheme of the reflectometer set-up envisaged for RTP. All numbers are frequencies in MHz, unless specified otherwise. PLL = phase-lock loop, LO = local oscillator, FM = frequency modulation.*

Table III: Specifications of the 12-channel reflectometer	
The design parameters of the proposed microwave reflectometer:	
Number of channels:	24 (12 high- and 12 low-field side)
Three instruments:	
Ka-band:	27, 33 and 39 GHz
U-band:	43, 47, 51, 55 and 59 GHz
E-band:	64, 72, 80 and 88 GHz
Resolution in fixed frequency mode	< 1/100 of the relevant wavelength
Sampling frequency in fixed freq. mode	up to 1 MHz
Resolution in stepped frequency mode	< 1 cm
Sampling frequency in step freq. mode	up to 100 kHz

Two modes of operation will be possible; a fixed frequency mode for detection of fast and relative movements of the critical density layer and a stepped frequency mode to measure the distance from the antenna to the critical density layer. A step in frequency (e.g. 100 MHz) will result in a phase shift which is a direct measure for this distance. This will be done in the following way: the LO frequency will be stepped from 3000 to 3010 MHz in, e.g. 100 μs. The phase-lock loop (PLL; see Fig. 13) will keep the frequency difference of the LO and the Gunn oscillators stable in the stepped frequency mode. This will force the Gunn oscillators to frequencies of 27105, 33130 and 39155 MHz, respectively.

III.3.3   Collective scattering diagnostics

Scattering of EM waves from electrons in plasmas can also provide information regarding the collective behaviour of scatterer electrons and ions shielded by them, e.g. the ion thermal distribution, electron density fluctuations, electrostatic plasma waves involving modulation of electron density such as ECRH waves and so on. In principle the frequencies and the wavenumbers of the probe (o), scattered (s), and the scatterer (w) waves or fluctuations satisfy the energy and momentum conservation:

$$\mathbf{k_s} - \mathbf{k_o} = \mathbf{k_w} \quad \text{and} \quad \omega_s - \omega_o = \pm \, \omega_w.$$

However, the detailed information content in the scattered radiation depends on the scattering configuration and plasma characteristics. The key parameter to classify different scattering regimes is the scattering parameter,

$$\alpha = (k_w \lambda_D)^{-1},$$

where $\lambda_D = (kT/4\pi n e^2)^{1/2}$ is the Debye length. When $\alpha \ll 1$ the scattered spectrum is determined by the individual electrons, whilst when $\alpha \gg 1$ it will be determined by the collective behaviour of electrons in a Debye sphere. For Bragg scattering, where $\omega_s = \omega_o$ and $|k_s| = |k_o|$ it follows $k_w = 2 \, k_o \sin \theta_s/2$, with θ_s the scattering angle. The scattering parameter can be recast as

$$\alpha = (2 \, \lambda_D \, k_o \sin \theta_s/2)^{-1}.$$

Therefore, the plasma parameters, probe wavelength and scattering angle determine the scattering regime. For collective scattering ($\alpha \gg 1$) where the scattered power is enhanced due to the cooperative scattering by many electrons, the appropriate wavelengths are typically in the microwave, FIR and IR region. Usually IR scattering with CO_2 lasers results in somewhat too small scattering angles of less than $1 - 2°$, while microwaves suffer refraction problems.

III.3.3.1   Collective scattering on microturbulence

For RTP, a FIR multichannel heterodyne collective scattering system for detailed measurement of plasma microturbulence (Fig. 14) is based on the twin-frequency FIR laser system already in use for the multichannel interferometer. The heterodyne detection capability of the system (intermediate frequency ≤ 1 MHz) will enable determination of the propagation direction of fluctuations up to ≈ 1 MHz. The high sensitivity of the mixers will permit detection of density fluctuations as small as $\tilde{n} = 10^{15}$ m^{-3}. The multichannel capability will permit a simultaneous measurement of 6 different wavenumbers ranging from $k_w = 4 - 40$ cm^{-1} and one extra channel for $90°$-scattering ($k_w = 100$ cm^{-1}). Hence, microturbulence spectra $\tilde{n}$ (k,ω) can be obtained as a function of time at each position inside the plasma. This data is crucial to evaluate various turbulent transport theories and thus will provide valuable insight into the mechanisms of anomalous transport in tokamaks. One of the detectors will be equipped with fast data-acquisition electronics to enable the measurement of fluctuations up to 100 MHz. Since the IF frequency of the twin-beam far-infrared laser is limited to a few MHZ one cannot use heterodyne detection techniques in this high-frequency range. Homodyne techniques have to be preferred instead for this channel.
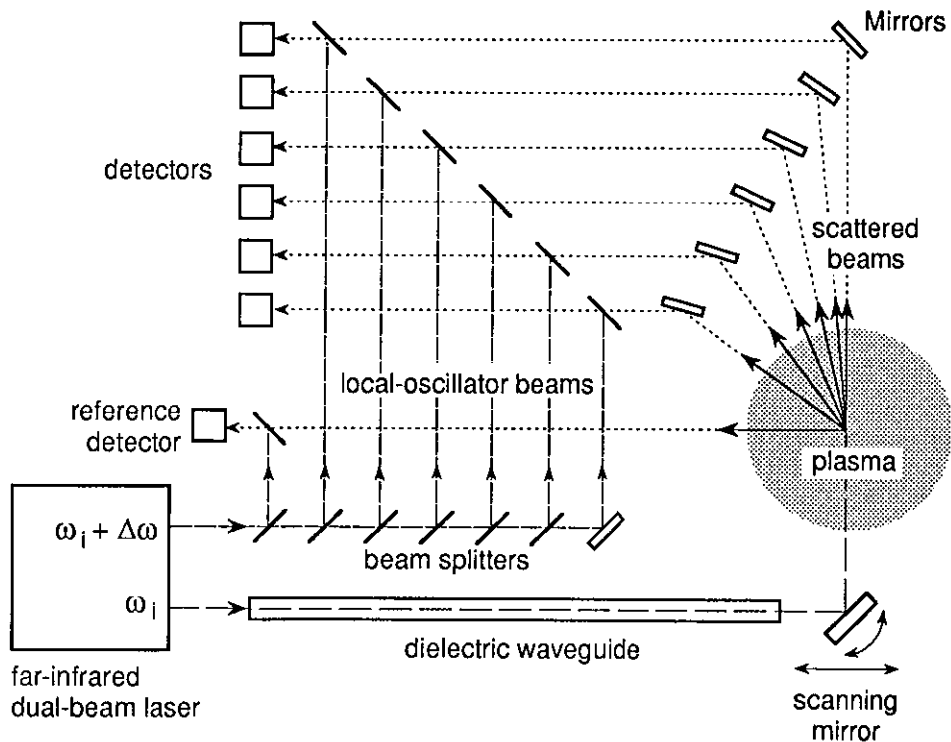

Fig. 14   Schematic lay-out of the collective scattering diagnostics system envisaged for RTP. The local oscillator beam can be shifted in frequency a few MHz by changing the length of the corresponding FIR cavity. The scattering volume can be positioned at any place in the plasma by changing the position and angle of the scanning mirror (the angles of the detection mirrors have to be changed simultaneously).

III.3.3.2   Collective scattering on ECR-induced density waves

Another collective scattering system slightly different from the above described system is proposed for RTP.[33] This system is for monitoring plasma-wave activities during
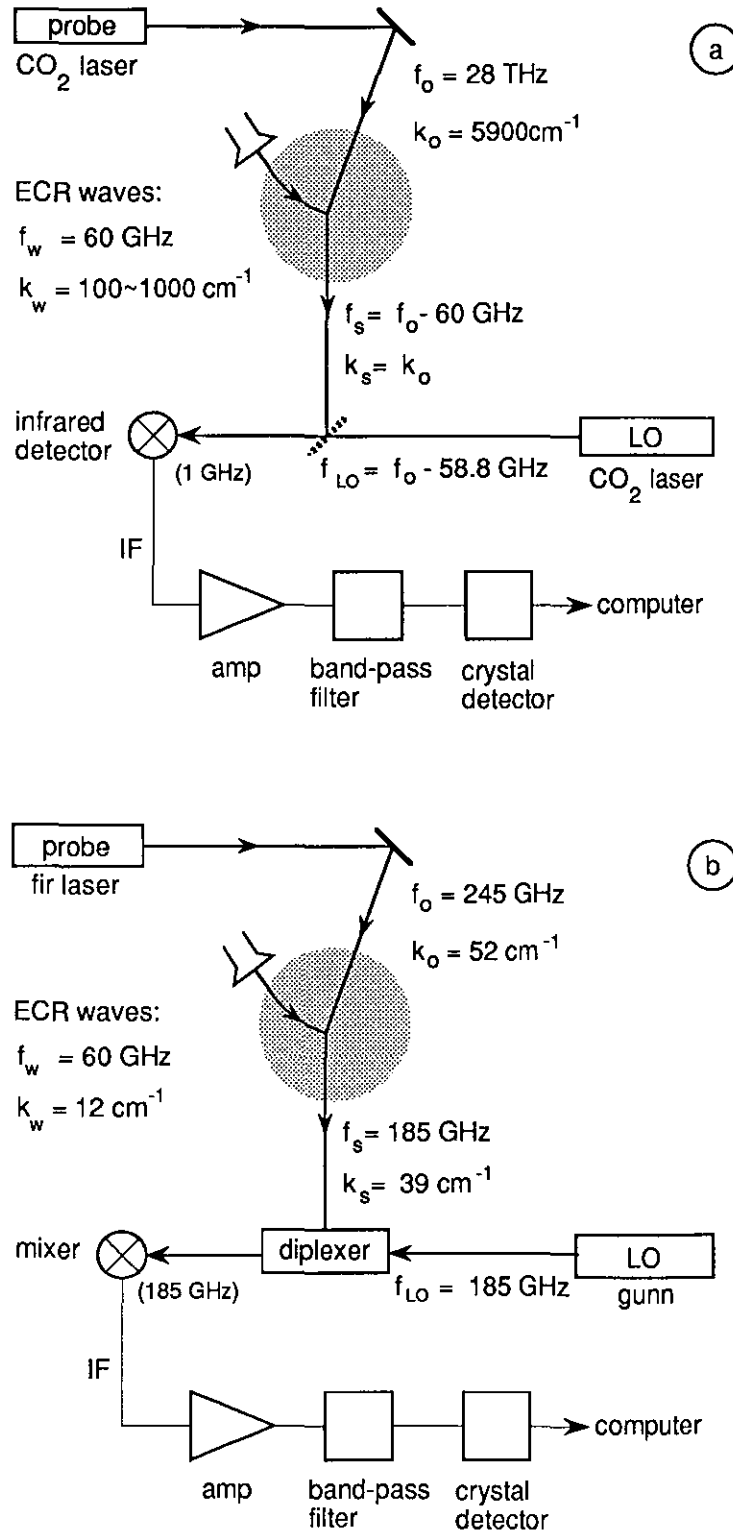

Fig. 15   Schematic drawing of the collective IR (a) and FIR (b) scattering diagnostics.

electron cyclotron resonance heating (ECRH). Since the frequency of the ECRF waves is very high (~ 60 GHz), a LO separated by 60 GHz in frequency from the probe is employed. For electron Bernstein wave measurement (k_w = 100 - 1000 cm^{-1}), both the probe and LO utilize CO_2 lasers (k_o = 6000 cm^{-1}; see Fig. 15a). These CO_2 lasers are each operating at one of the two adjacent lines to produce the required frequency difference of ~ 60 GHz. For X-mode pump waves, the probe will be the FIR laser operating at 245 GHz (1.2 mm) and the LO will be a 185 GHz solid-state Gunn oscillator (see Fig. 15b). This 245 GHz scattering can be combined with the microturbulence scattering by separating signals scattered from microturbulence (~ 245 GHz) using frequency-selective filters (called diplexers), allowing simultaneous measurement of ECR-induced density waves and other density fluctuations and therefore direct effects of ECRH on the plasma transport.

III.4   Particle diagnostics

III.4.1   Neutral particle analysis (passive and active)

In the first instance the ion temperature on RTP will be measured by means of passive neutral particle analysis. This measurement delivers the line-integrated ion temperature in the plasma, strongly weighted towards the cold plasma edge.[34] The central temperature, however, can also be deduced from the measurements by looking at the tail of the measured energy distribution.
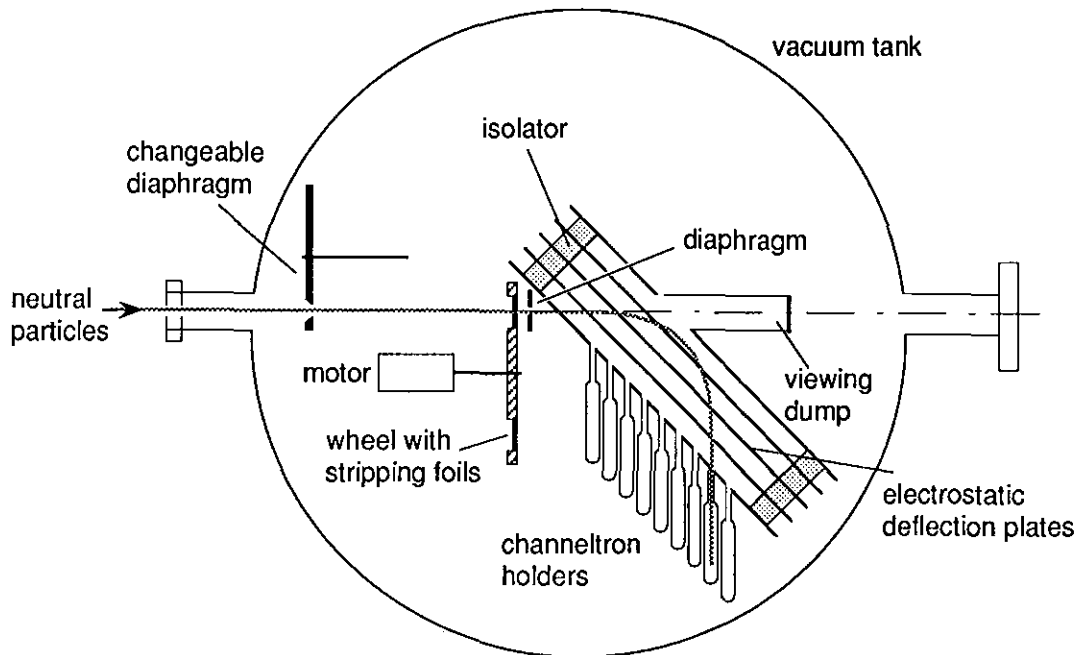

Fig. 16   Cross-sectional view of the 8-channel electrostatic neutral particle analyser.

The energy distribution of the neutrals escaping from the plasma is determined by means of electrostatic analysis. Neutrals from the plasma are stripped of their electrons by an ultra-thin carbon foil with a thickness of 1 $\mu g/cm^2$, corresponding to about 5 nm. The ions coming out of the foil enter an electrostatic analyser consisting of two parallel plates at an angle of 45° to the incoming beam (see Fig. 16). Eight channel electron multipliers are used to measure the number of ions at each energy.

A stripping foil was chosen instead of a stripping cell, since the first one has a much higher (about a factor 5 - 10) conversion efficiency.[35,36] The deterioration of the energy resolution of the detector due to angular and energy straggling in the foil is found to be minimal. Furthermore, due to the higher sensitivities at higher energies, the detector becomes much more sensitive to the tail distribution and, hence, to the central ion temperature.[34] A possible future extension of the analyser could be the detection of secondary electrons emitted by the stripping foil.[37] This would enable a time-of-flight measurement by determining the time the particle needs to travel from the stripping foil to one of the channeltrons. This additional information would allow the diagnostician to determine not only the energy but also the mass of the detected particle, using only one array of channeltrons.

In addition, a diagnostic beam will be implemented on one of the top ports, to inject a beam of He- or H-neutrals vertically through the centre of the plasma. The total density of neutral particles in the plasma core will thus be increased by this and, hence, the number of charge exchange neutrals emerging from the plasma centre and detected by the analyser will be larger than in the passive measurement.[38] The energy of the neutrals is 20-25 keV at an equivalent neutral beam current of 50 mA.

A special time-of-flight analyser was developed at Rijnhuizen for the detection of neutrals with very low energies emitted by the extreme plasma edge.[39] The detection technique is based on the conversion of neutral atoms into negative ions. The charge conversion takes place on a mono-crystalline tungsten surface covered with a mono-layer of cesium.

The time-of-flight analyser (Fig. 17) consists of a chopper disk, a flight tube and a detector housing. After passage through the tube, the neutrals will hit a cesiated tungsten surface in the vacuum chamber (Fig. 18). After acceleration the resultant H⁻-ions are detected by a channeltron which has to be mounted in a box to prevent it from being covered with cesium during or shortly after the dispenser activation period.

The first measurements have been performed on the TORTUR tokamak.[40] Figure 19 is an example of what a typical time-of-flight spectrum from the TORTUR plasma looks like. The time-of-flight spectrum in Fig. 19 is the result of adding 104 subsequent spectra obtained during the flat and reproducible plateau phase of a single TORTUR discharge, taking the chopper open time as a reference signal. The adding up has been done for statistical reasons.
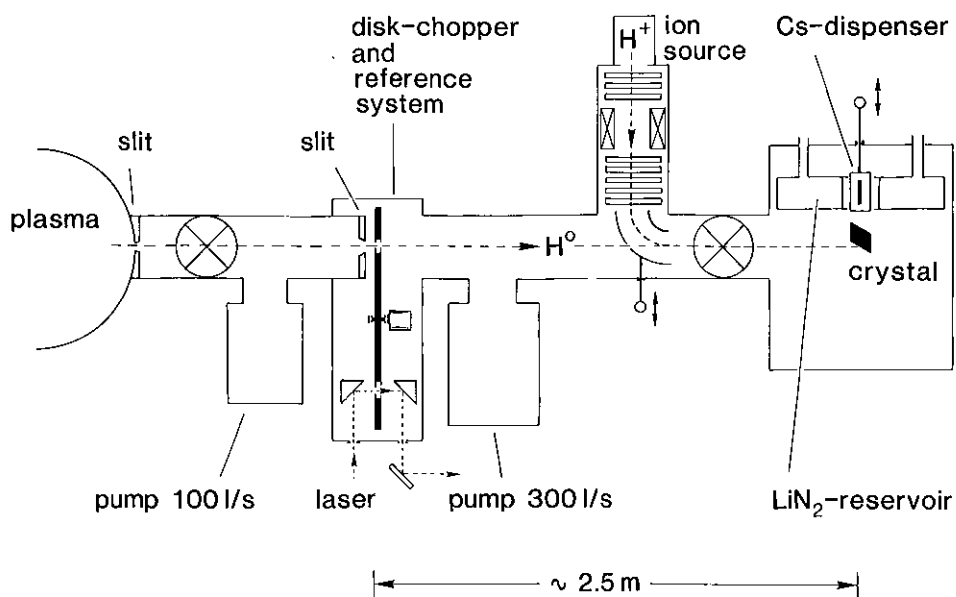
Fig. 17   *Schematic overview of the time-of-flight analyser for low-energetic neutrals.*
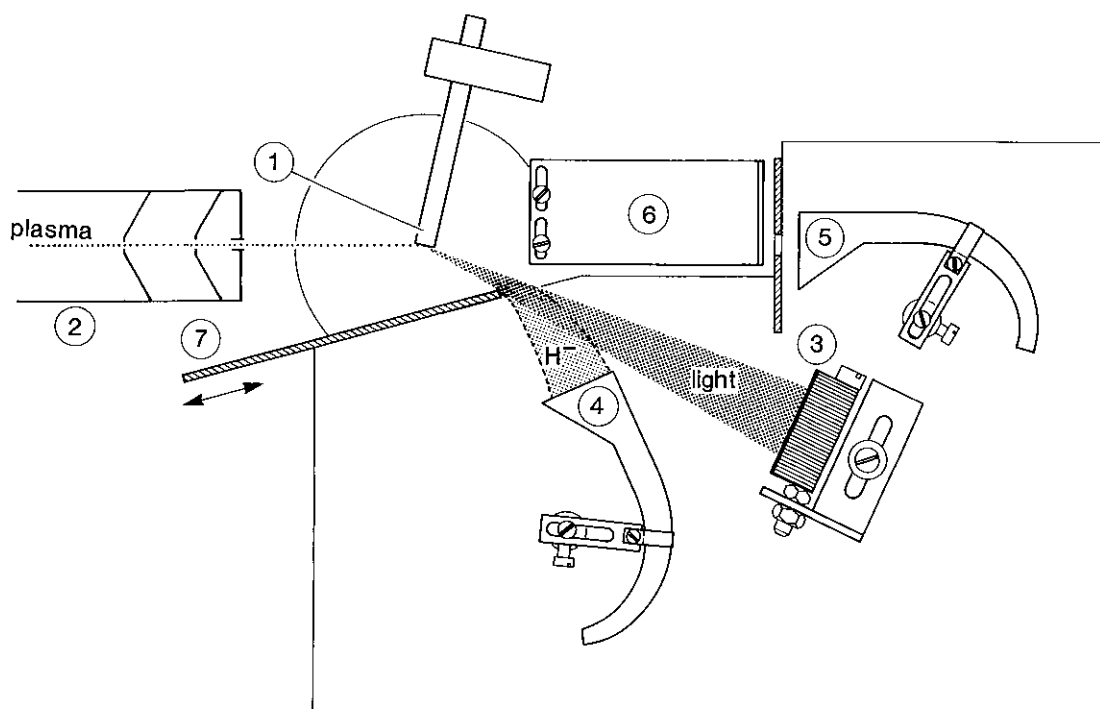

Fig. 18   *The scattering chamber of the time-of-flight analyser: (1) tungsten crystal, (2) collimator, (3) razor-blade light dump, (4,5) channeltrons and (6,7) moveable shutters.*

The small number of slits in the chopper disk and consequently the long duration of a single spectrum enables a clear distinction between plasma signal and background. The latter consists of noise from cesium and cesium-induced electronic emission, and X-rays from the plasma. The double peak structure of the spectrum can be attributed to the distinct contributions from the interior and the edge of the plasma.
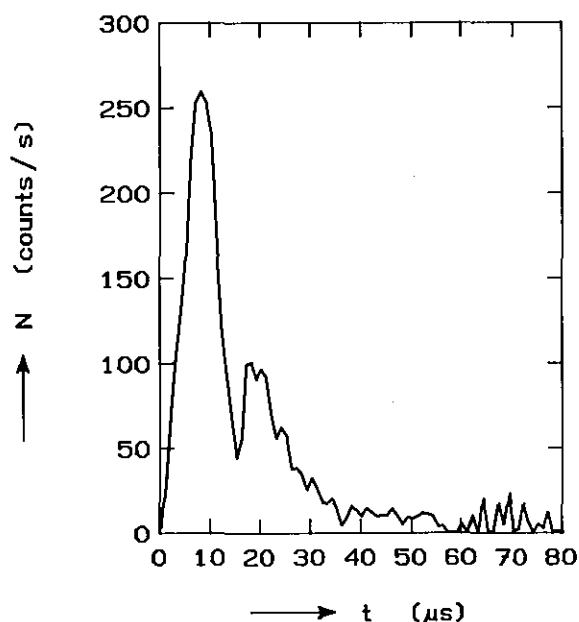

Fig. 19 Time-of-flight spectrum of low-energetic neutrals emerging from the TORTUR tokamak.

The X-ray induced background has been minimized by constructing the chopper disk out of 1 mm thick stainless steel. During the open time of the chopper, however, no hard X-rays were detected. Therefore, the spectrum in Fig. 19 is totally determined by the particle flux from the plasma. The spectrum is corrected for the background and cut off at 60 μs.

III.4.2   Charge exchange recombination spectroscopy

Once the diagnostic beam is implemented it will also be used to deduce the ion temperature from charge exchange recombination reactions. The electrons which are captured by the plasma ions generally end up in the excited states of the neutral. When they fall back to the ground state, photons are emitted. Measurement of the spectrum of emitted photons by means of an optical multichannel array enables the deduction of the local ion temperature from the line widths, which are broadened by the thermal motion of the ions.[41,42]

III.4.3   Rutherford scattering

Small-angle elastic scattering of light neutrals from the diagnostic beam by plasma ions can be used as a diagnostic method to attain a spatially and temporally resolved measurement of the ion temperature.[43,44] After a single Rutherford scattering, the fast neutrals carry information about the local ion-velocity distribution. The value of the ion temperature can be deduced from the width of the observed energy distribution of scattered particles in a direct manner and without the necessity of making assumptions (see Fig. 20).
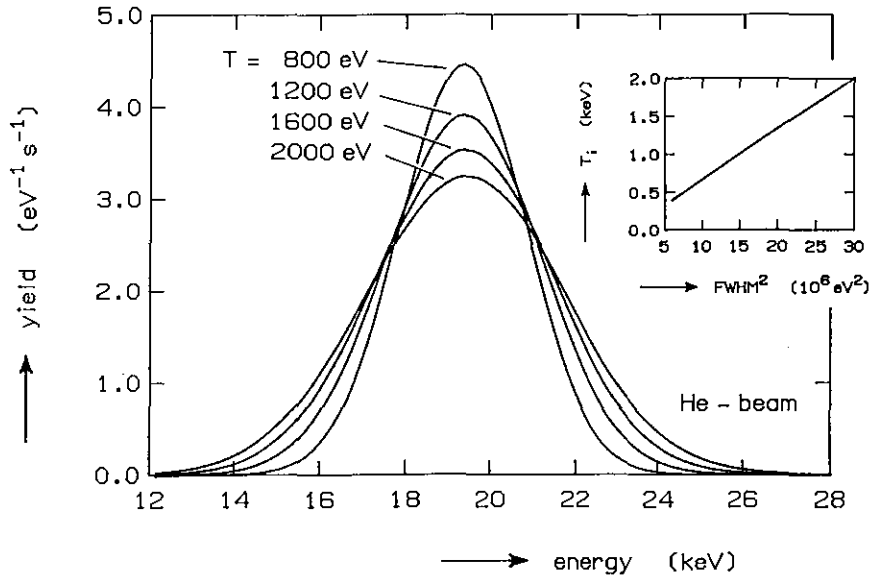

Fig. 20   *Calculated scattering distribution for several values of the local ion temperature T in case of a neutral He-beam, at a scattering angle of 5°. The inset shows the dependence of the FWHM of the distribution on T.*

The essential components for a Rutherford-scattering experiment are a mono-energetic diagnostic beam of hydrogen or helium atoms and an (time-of-flight) analyser with high energy resolution. The diagnostic beam should be directed vertical to the equatorial plane towards the axis of the plasma column. The observation angle should be chosen at an angle of 5° to 10° with respect to the beam axis. A special time-of-flight analyser was constructed at Rijnhuizen featuring a triple-coincidence detection technique, to attain a low sensitivity to gamma-radiation.[44]

Feasibility studies where performed for implementation of the time-of-flight analyser promise high counting rates (i.e. good accuracy), high temporal resolution and low sensitivity to highly-charged impurities in the plasma. The expected accuracy in the temperature measurement will be 10% or better.

III.5 Spectroscopic diagnostics

III.5.1 Visible light and X-ray tomography

Two tomography diagnostics, each concerning a different part of the electromagnetic spectrum, will be situated at the same toroidal location. X-ray tomography will cover the energy range from 1 to 30 keV (0.04 to 1.2 nm), whereas visible light tomography ranges from about 1.7 to 3.5 eV (350 to 700 nm). The purpose of both diagnostics is to resolve fluctuations in the plasma emissivity with good spatial ($\approx$ 1- 2 cm) and temporal ($\approx$ 2 μs) resolution. These fluctuations might be related to transport phenomena and sawtooth behaviour.

The main purpose of the soft X-ray tomography system is the study of MHD modes. With the system under development for RTP, it will be possible to detect MHD oscillations of m-number up to 4 without assuming any plasma rotation. A total of five small pin-hole cameras with 16 detectors each in one poloidal plane will be employed. The cameras will be positioned inside the vacuum vessel and as close as possible to the plasma (20 cm from the plasma centre) in order to increase the signals and to facilitate viewing angles which cannot be reached if the cameras would be mounted outside the vessel. Due to the narrow width of the vertical ports the cameras have to be very compact. A set-up similar to that of Alcator-C[45] was chosen. The high baking temperatures of the RTP vacuum vessel necessitates cooling of the cameras with nitrogen gas. The positions of five cameras with respect to the plasma are indicated in Fig. 21a. The spatial coverage of the detector's line-of-sight is indicated in the p–φ diagram of Fig. 21b. The tomographic reconstruction of the plasma emission can be done only for the region within 12 cm from the plasma centre.

Each detector measures the line integral of the emissivity along its viewing line. The reconstruction of the local emissivity will be done by using two tomographic reconstruction methods: an analytical method and a hybrid method.[46] The first method, developed by Cormack, decomposes the 2-D functions (of angle and radial position) into their harmonics, transforming the 2-D integral in a set of 1-D integrals that can be inverted thereafter.[47] The second method, developed by Smeulders, divides the plasma into pixels that approximate the magnetic flux contours (annular pixels in the case of RTP), allowing the emissivity within a pixel to vary in the annular direction. The angular variation of the emissivity is then expanded in Fourier components, whose number is consistent with the number of cameras.[48]
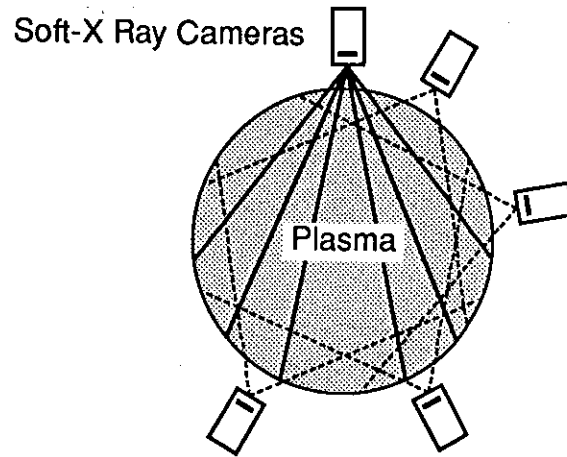
Fig. 21a   Geometrical arrangement of the five pinhole cameras around the RTP plasma.
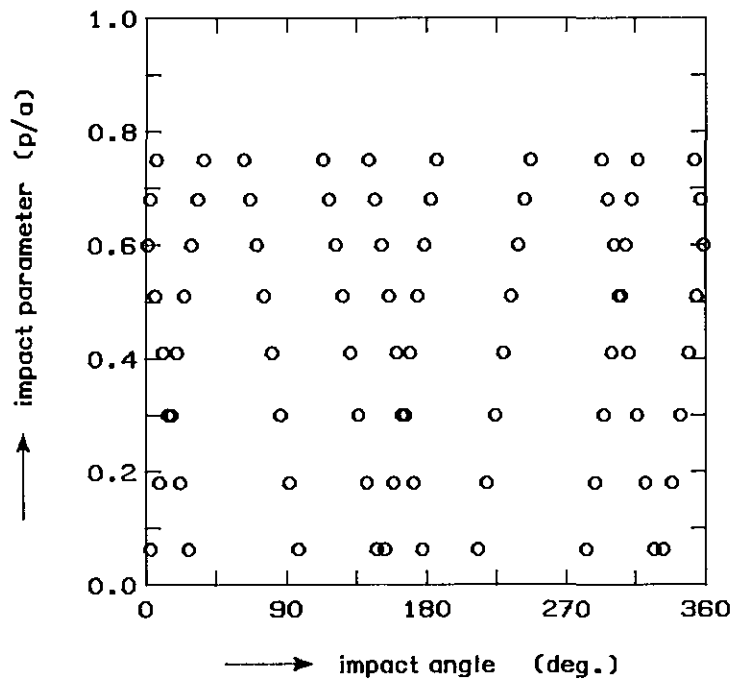

Fig. 21b   Spatial coverage of the plasma given in a p-φ diagram.

For visible light tomography, which will be especially dedicated to studies of Z_{eff}-profiles,[49] impurity ion distributions,[50] H_α-emission, ion temperature measurements and the occurrence of filamentation in the plasma, it is planned to position the detectors outside the vacuum vessel. The difference from other conventionally used tomographic diagnostics is the optical imaging. Three cameras will use first-surface coated parabolic mirrors, and one camera will be equipped with lenses. In the provisional design, much care is taken primarily to obtain the optimum number of photons and hence, the time resolution of the system. Furthermore, large solid angles can be used, still retaining a good spatial resolution. Filtering can be done

outside the vacuum and offers the opportunity to investigate discrete lines (H_α) or bremsstrahlung.

The reconstruction of the visible light tomography data will be carried out with the two methods mentioned above and with the maximum entropy method[51] in order to investigate which method gives the best resolution at the edge of the reconstructed plasma emissivity profile. It is expected that filamentations in the image plane with a dimension as small as 10 mm in the poloidal direction can be detected.
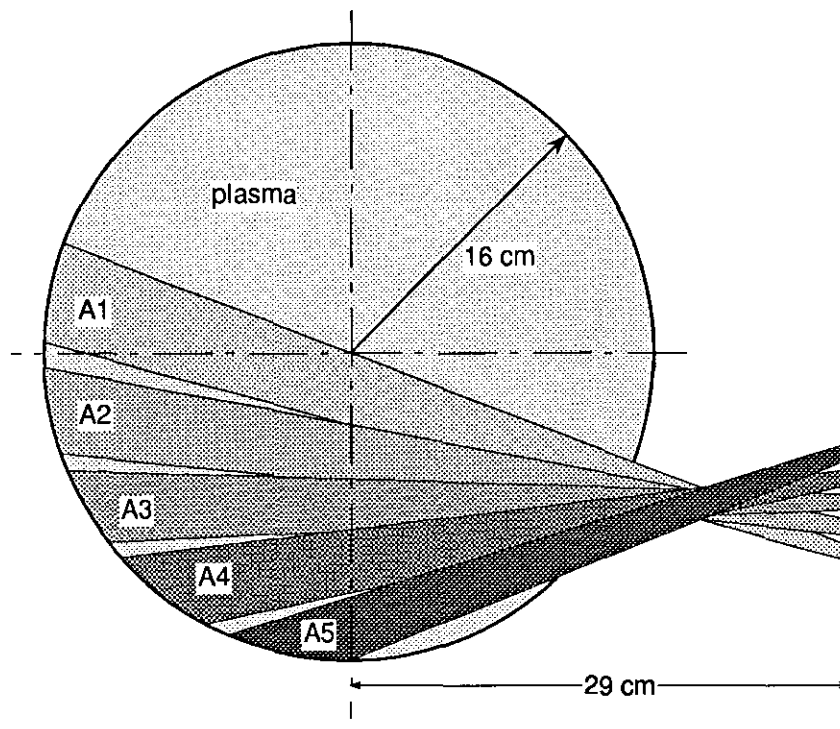

Fig. 22   Location of the five viewing lines in the preliminary visible light measurements at RTP.

Preliminary measurements of the visible light emission at RTP are presently being performed. Five lines-of-sight (see Fig. 22) are used, viewing the lower half of the poloidal plane. Preliminary measurement results during RTP gas discharges and a reconstruction of the measurements, assuming rotational symmetry of the plasma, are shown in Figs. 23 a and b.

Moreover, the visible light spectrum is being recorded with the aid of a Bentham spectrometer and an optical multichannel analyser, the combination of both having a dispersion of 30 pm/channel. On the one hand, the spectrum indicates which impurities and charge-exchange lines are present in the plasma. On the other hand, line-free parts of the visible light spectrum can be observed. The intensity of radiation in these regions can yield the Z_{eff} of the plasma.
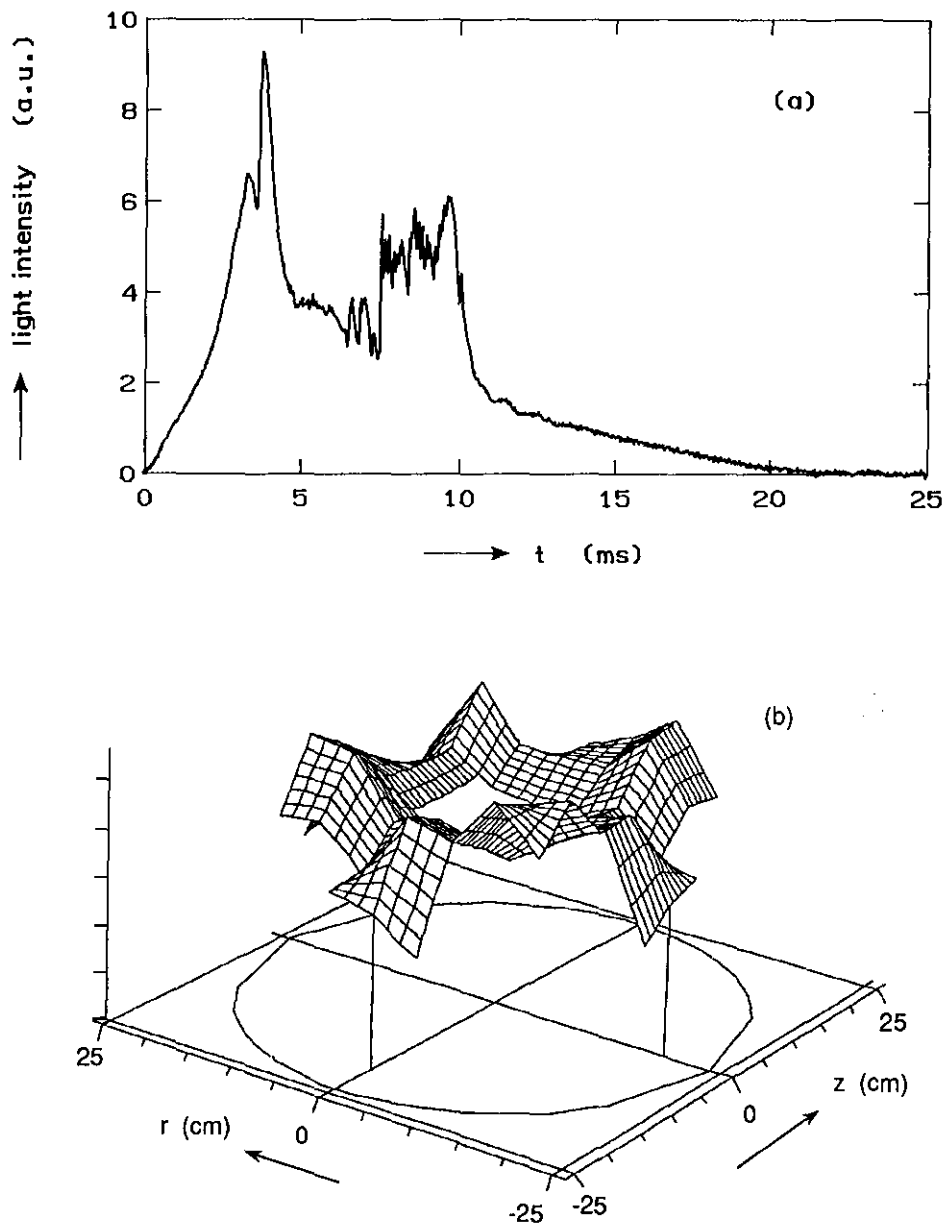
Fig. 23   (a) Time development of the integrated visible light signal measured during a RTP gas discharge (I_p = 20 kA). From filter measurements it is estimated that 25% of the emission is in the infrared ($\lambda \geq 780$ nm) and 50% is H_α line emission (λ = 656.3 nm). 100 mV corresponds with an emissivity of about 10^{20} photons $s^{-1}m^{-3}$. The plasma current starts at t = - 6 ms.

(b) The maximum entropy tomographic reconstruction indicates, under rotation symmetry assumptions, that the gas-discharge emissivity profile is hollow (arbitrary scales). After calibration, chord A1 was found not to view through the middle of the plasma. Therefore, no emissivity is shown in the centre of the reconstruction.

III.5.2   X-ray pulse height analysis

The electron energy distribution in the parallel direction as well as a value for Z_{eff} can be deduced from measurements performed with a soft X-ray pulse height analysis system. A SiLi-type detector is used in conjunction with beryllium absorber foils with various thicknesses (see Fig. 24). In the first instance, a very simple system will be manufactured, featuring a gas attenuation cell and diaphragm/foil combination which can be changed in between two RTP discharges. The detector will observe the plasma along a tangential viewing chord.
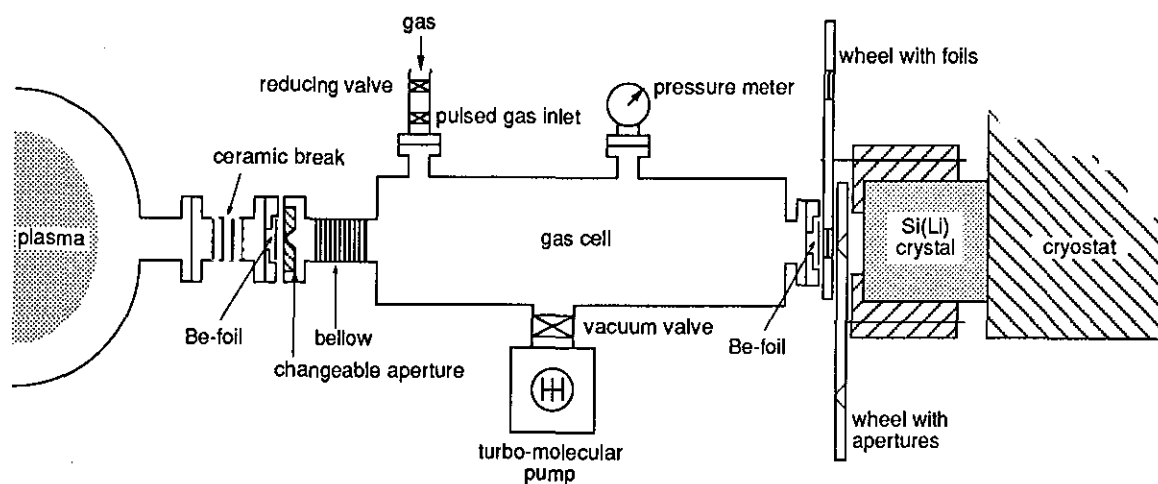

Fig. 24   Schematic diagram of the soft X-ray pulse height analysis system.

The presence of non-thermal electron populations will be detected by means of a hard X-ray pulse height analysis system. This will give indication during periods of rapid particle transport, for example due to plasma instabilities.

III.5.3   XUV, VUV and visible light spectroscopy

Plasma emission in the XUV, VUV and visible light regions will be monitored by various spectrometers (see Table IV). The main purpose of these measurements will be the deduction of the impurity contents of the plasma (Z_{eff}-measurement), impurity-ion temperatures from line broadening, etc. Especially since the visible light tomography system will not be used for each plasma shot (since the electronic circuitry and the data acquisition are shared with X-ray tomography), it is useful to have an impurity monitor in those shots where visible light tomography is absent. Furthermore, since visible light tomography focuses on only a part of the spectral region, VUV and XUV spectrometry are worthwhile to be operated for monitoring

Table IV : Specifications of the VUV-spectrometers

1] Hilger and Watts 480E (Rowland mount)

Angle of incidence		2°
Gratings:	cylindrical, ruled, gold coated	
	R	2000 mm
	d^{-1}	576 mm^{-1}
	λ_{blaze}	5 nm
Spectral range:		
	photographic mode:	0 - 125 nm
	photo-electric mode (2 channels):	1.5 - 105 nm
Typical resolution		0.02 nm

2] Jobin Yvon HR 1500 (Czerny-Turner)

Focal length		1500 mm
Aperture		f/12
Grating:	BaF$_2$-coated, holographic	
	d^{-1}	3600 mm^{-1}
	λ_{blaze}	160 nm
Spectral range		100 - 400 nm
Monochromator mode: resolution ($\Delta\lambda/\lambda$)		$\geq 10^5$
Polychromator mode:		
	number of channels	20
	typical channel width	0.015 nm
	typical channel separation	0.015 nm

3] Jobin Yvon LHT 30

Focal length		320 mm
Aperture		f/10
Grating:	toroidal, holographic	
	d^{-1}	550 mm^{-1}
Spectral range		15 - 150 nm
typical resolution $\Delta\lambda$		0.4 nm
Polychromator mode:		
	number of channels	20
	typical channel width	0.015 nm
	typical channel separation	0.015 nm

purposes. The spectrometers can also be used to obtain information about forbidden lines, which are of interest for atomic physicists.

In the visible region a detailed analysis of certain spectral lines can give some additional plasma information. As the Stark broadening of the H_α and H_β lines at an electron density of 10^{19} m^{-3} is 0.01 nm or less, the neutral temperature can be derived from the Doppler-broadening of one of these spectral lines (typically 1 nm at 1 keV). Furthermore, the ion temperature can be evaluated in the same way by analysing impurity-ion lines (e.g. CII-IV, OII-VI, etc.).

III.5.4 Bolometry

The integrated radiation loss from the RTP plasma will be measured by a radiative bolometer.[52] The detector is specifically designed to respond to the total radiative energy flux with a spectral response as flat as possible in the soft X-ray and ultraviolet regions of the spectrum, in which the major radiative loss from the plasma will occur. The bolometer will consist of a 6 µm thick platinum absorbing foil, positioned in the scrape-off layer and designed to absorb all the incident energy. A constant offset is given to the temperature of the foil by means of a highly stable power supply. This is done to get the foil into the infrared radiative region. Radiation from the plasma will result into an additional temperature rise of the foil, equal to the total energy flux divided by the bolometer's thermal capacity. The radiative temperature of the absorber foil is measured by means of a fibre-optically coupled detector positioned far from the tokamak to avoid electronic pick-up.

A special calibration unit will be built featuring a pulse generator with well-known current and pulse duration (the latter proportional to the length of the RTP pulse). The voltage over the foil will be measured by means of a bridge circuit.

IV   Data acquisition

For the RTP experiment a new data-acquisition system is being developed. The central part is a distributed computer system. It consists of 25 MC68030-based CPU-boards. Each of these processor boards has a transient recorder (data recording unit) attached to it. Each transient recorders is equipped with eight 12-bit AD-converters and 4 Mbyte of recording memory. These recorders are especially designed for our Institute. The total system is capable of recording 200 signals at a sampling rate of 1 MHz during the entire plasma phase (≤ 250 ms). When the discharge is finished the total processing power (up to 100 MIPS and 10 MFLOPS) is available for data reduction and on-line analysis. Finally, a reduced number ($n \leq 10^6$) of the data is transferred to the central computer system, where it is stored. The stored data will be available for several years and are accessible to all users.

Research items involved in the development of the above data-acquisition system are:
- the managing of a distributed system in a real time environment,
- the development of appropriate data-reduction methods and
- the development of distributed algorithms.

V   Conclusion

The RTP tokamak is presently being commissioned. The primary research aim of the Rijnhuizen Tokamak Project is the study of transport and fluctuations in tokamak plasmas. This has led to a choice for diagnostics featuring high accuracy and good spatial and temporal resolution. In the first phase of RTP those diagnostics which were previously used at other plasma devices at Rijnhuizen will be implemented. In a later phase totally new diagnostics will be developed and implemented. The RTP diagnostics which were described in this report are expected to be operational at the end of 1990 (with possibly a few exceptions depending on the availability of additional funding).

References

1   J. Wesson, Tokamaks, Clarendon Press, Oxford (1987).

2   P.C. Liewer, Nucl. Fusion 25 (1985) 543.

3   A.G.A. Verhoeven, H. Duit, P. Manintveld, R.W. Polman, F.M.A. Smits and A. Yildirim, Proc. Joint IAEA Techn. Comm. Meeting on ECE and EC-7 Meeting, Hefei, China, 1989, to be published.

4   F.M.A. Smits, Proc. Joint IAEA Techn. Comm. Meeting on ECE and EC-7 Meeting, Hefei, China, 1989, to be published.

5   H. de Kluiver, C.J. Barth and A.J.H. Donné, Plasma Phys. and Controlled Fusion 30 (1988) 699.

6   A.A.M. Oomens, to be submitted to Nucl. Fusion.

7   C.J. Barth and A.J.H. Donné, Proc. 3rd Symp. on Laser-Aided Plasma Diagnostics, Los Angeles (1987) p. 161.

8   C.J. Barth, Appl. Opt. 27 (1988) 2981.

9   C.J. Barth and D. Oepts, Appl. Opt. 27 (1988) 3838.

10 A.C.A.P. van Lammeren, C.J. Barth, A.J.H. Donné, Q.C. van Est and G.C.H.M. Verhaag, Proc.16th Eur. Conf. on Controlled Fusion and Plasma Phys., Venice (1989) Vol. IV, p. 1481.

11 R. Bartiromo, P. Buratti, L. Pieroni and O. Tudisco, Proc. 9th Eur. Conf. on Plasma Phys. and Controlled Fusion, Oxford (1979) p. 47.

12 M.A. Blokh and N.F. Larionova, Sov. J. Plasma Phys. 7 (1981) 31.

13 L. Pieroni and S.E. Segre, Phys. Rev. Lett. 34 (1975) 928.

14 U. Tartari, FP-84/20 (1984).

15 C.J. Barth, Rijnhuizen Report, to be published.

16 F. Alladio and M. Martone, Phys. Lett. 60A (1977) 39.

17 C.J. Barth, Rev. Sci. Instrum. 60 (1989) 2673.

18 I.H. Hutchinson, Principles of Plasma Diagnostics, Cambridge University Press, Cambridge (1987).

19 A.E. Costley, R.J. Hastie, J.W.M. Paul and J. Chamberlain, Phys. Rev. Lett. 33 (1974) 758.

20 M. Bornatici, R. Cano, O. de Barbieri and F. Engelmann, Nucl. Fusion 23 (1983) 1153.

21 R.M.J. Sillen, H.W. Piekaar, Th. Oyevaar and W. Werner, Infrared Phys. 24 (1986) 511.

22 R.M. Niestadt, Rijnhuizen Report 83-148 (1983).

23 R.M.J. Sillen, H.W. Piekaar, Th. Oyevaar, E.P. Gorbunov, A.A. Bagdasarov and N.L. Vasin, Nucl. Fusion 26 (1986) 303.

24 R.M. Niestadt, B.J.D. Tubbing and Th. Oyevaar, Rijnhuizen Report 86-168 (1986).

25 B.J.D. Tubbing, N.J. Lopes Cardozo and M.J. van der Wiel, JET Report JET-P 87-12 (1987).

26 M. Verreck, C.A.J. Hugenholtz and A. Pauw, Proc. Joint IAEA Techn. Comm. Meeting on ECE and EC-7 Meeting, Hefei, China, 1989, to be published.

27 I.H. Hutchinson and K. Kato, Nucl. Fusion 26 (1986) 179.

28 W.M. Kelly, D.R. Vizard, A.J.H. Donné, A.C.A.P. van Lammeren and S.K. Kim, Mikrowellen and HF Magazin 15 (1989) 249.

29 H. Soltwisch, Proc. Int. School on Plasma Phys.: Basic and Advanced Diagnostic Techniques for Fusion Plasmas, Varenna (1986) Vol. II, p. 343.

30 D.V. Bartlett, Proc.15th Eur. Conf. on Controlled Fusion and Plasma Phys., Dubrovnik (1988) Vol. III, p. 1119.

31 C.A.J. Hugenholtz and A.J. Putter, Rijnhuizen Report 86-170 (1986).

32 R. Prentice, Proc.15th Eur. Conf. on Controlled Fusion and Plasma Phys., Dubrovnik (1988) Vol. III, p. 1115.

33 S.K. Kim, C.A.J. Hugenholtz, A.J.H. Donné, W.A. Peebles and N.C. Luhmann Jr., Proc.16th Eur. Conf. on Controlled Fusion and Plasma Phys., Venice (1989) Vol. IV, p. 1473.

34 C.R. Parsons and S.S. Medley, Plasma Phys. 16 (1974) 267.

35 Yu.V. Gott and A.G. Motlich, Nucl. Instrum. Methods 155 (1978) 443.

36 P. Beiersdorfer, A.L. Roquemore and R. Kaita, Rev. Sci. Instrum. 58 (1987) 2092.

37 W.A. de Zeeuw, H.W. van der Ven and A.J.H. Donné, to be published in Rev. Sci. Instrum.

38 H.J.B.M. Brocken, Rijnhuizen Report 81-137 (1981).

39 W. van Toledo, H.J. van der Meiden, J.J.C. Geerlings and P.W. van Amersfoort, Phys. Lett. A119 (1986) 126.

40 W. van Toledo, A.R. de Bree, R. van Buuren, H. de Kluiver and A.J.H. Donné, Proc.16th Eur. Conf. on Controlled Fusion and Plasma Phys., Venice (1989) Vol. IV, p. 1485.

41 A. Boileau, M. von Hellerman, W. Mandl, H.P. Summers, H. Weisen and A. Zinoviev, J. Phys. B: At. Mol. Phys. 22 (1989) L145.

42 M. von Hellermann, A. Boileau, L. Horton, W. Mandl, H.P. Summers and H. Weisen, Proc.16th Eur. Conf. on Controlled Fusion and Plasma Phys., Venice (1989) Vol. I, p. 107.

43 V.G. Abramov, V.V. Afrosimov, I.P. Gladkovskii, A.I. Kislyakov and V.I. Perel', Sov. Phys. Tech. Phys. 16 (1972) 1520.

44 A.J.H. Donné, E.P. Barbian and H.W. van der Ven, J. Appl. Phys. 62 (1987) 3130.

45 J.F. Camacho and R.S. Granetz, Rev. Sci. Instrum. 57 (1986) 417.

46 R.S. Granetz and P. Smeulders, Nucl. Fusion 28 (1988) 457.

47 A.M. Cormack, J. Appl. Phys. 35 (1964) 2908.

[48] P. Smeulders, Nucl. Fusion 26 (1986) 267.

[49] H. Röhr, K.H. Steuer and the ASDEX team, Rev. Sci. Instrum. 59 (1988) 1875.

[50] K. Kadota, M. Otsuka and J. Fujita, Nucl. Fusion 20 (1980) 209.

[51] A. Holland and G.A. Navratil, Rev. Sci. Instrum. 57 (1986) 1557.

[52] Yu.G. Prokhorov, Sov. Phys. Dokl. 5 (1960) 1048.